

EPR Spectroscopy

Spying on unpaired electrons - What information can we get?



Sunrise Free Radical School
Oxygen-2002 :: Nov 21, 2002

Periannan Kuppusamy, PhD

Center for Biomedical EPR Spectroscopy &
Imaging

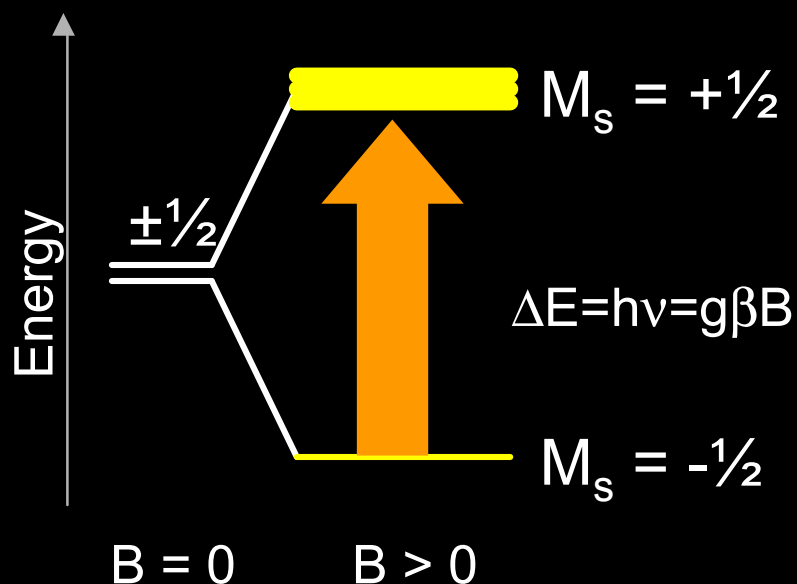
Davis Heart & Lung Research Institute

Ohio State University, Columbus, OH

E-mail: Kuppusamy.1@osu.edu

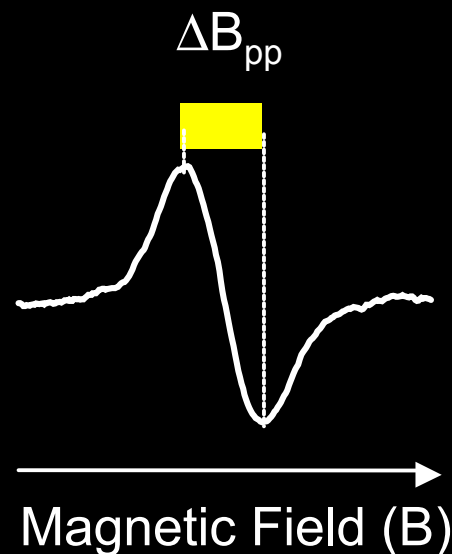
What is EPR?

Electron Paramagnetic Resonance (EPR)
Electron Spin Resonance (ESR)
Electron Magnetic Resonance (EMR)
EPR ~ ESR ~ EMR



h Planck's constant 6.626196×10^{-27} erg.sec
 ν frequency (GHz or MHz)
 g g-factor (approximately 2.0)
 β Bohr magneton (9.2741×10^{-21} erg.Gauss $^{-1}$)
 B magnetic field (Gauss or mT)

EPR is the resonant absorption of microwave radiation by paramagnetic systems in the presence of an applied magnetic field



$$h\nu = g\beta B$$

$$\nu = (g\beta/h)B = 2.8024 \times B \text{ MHz}$$

for $B = 3480$ G

$\nu = 9.75$ GHz (X-band)

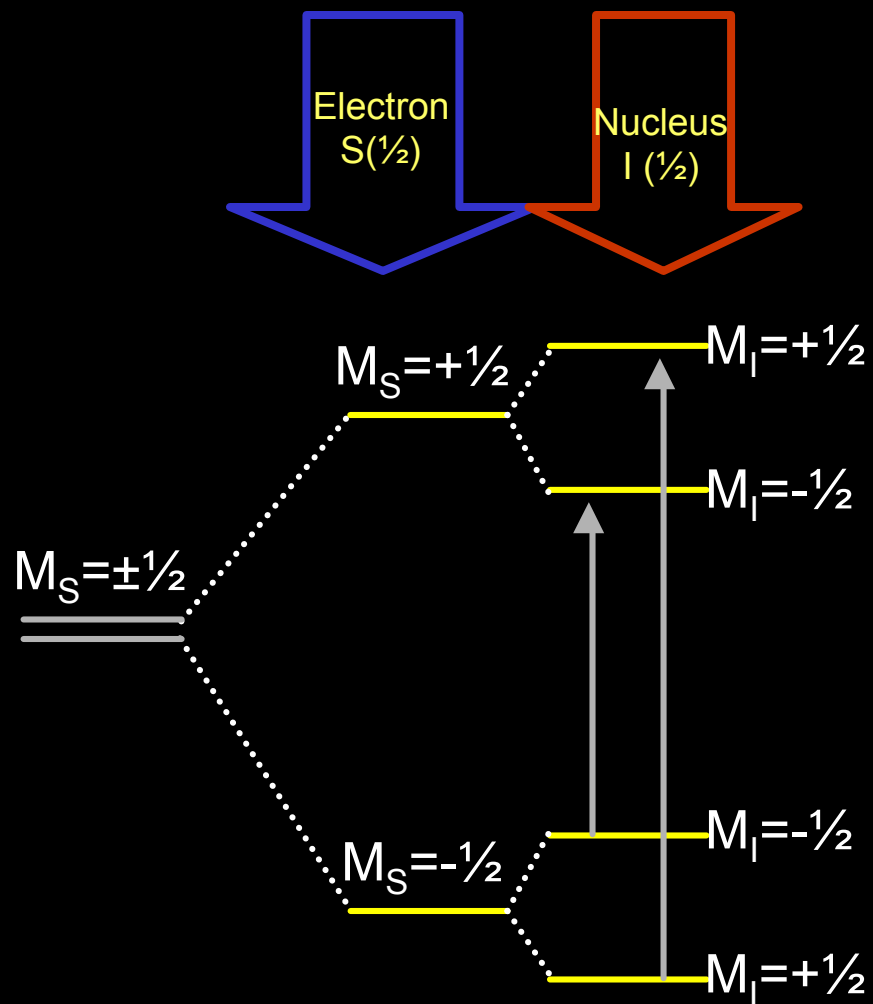
for $B = 420$ G

$\nu = 1.2$ GHz (L-band)

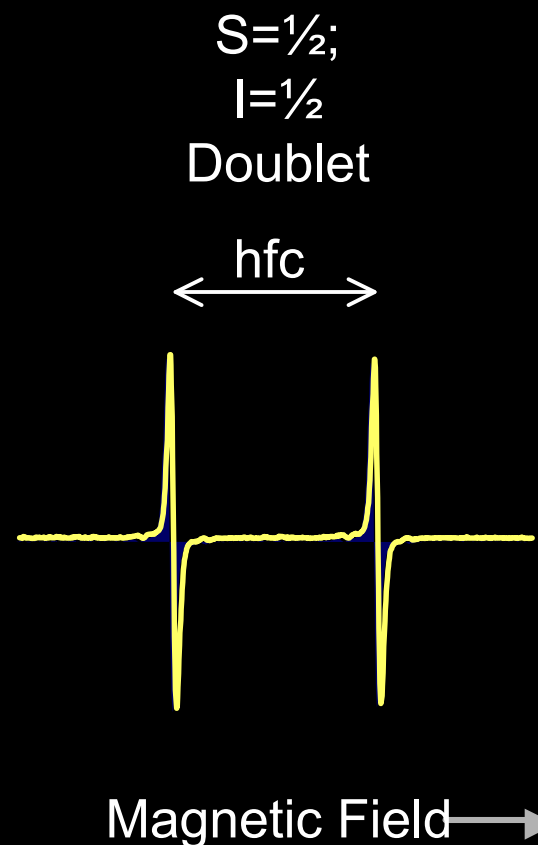
for $B = 110$ G

$\nu = 300$ MHz
(Radiofrequency)

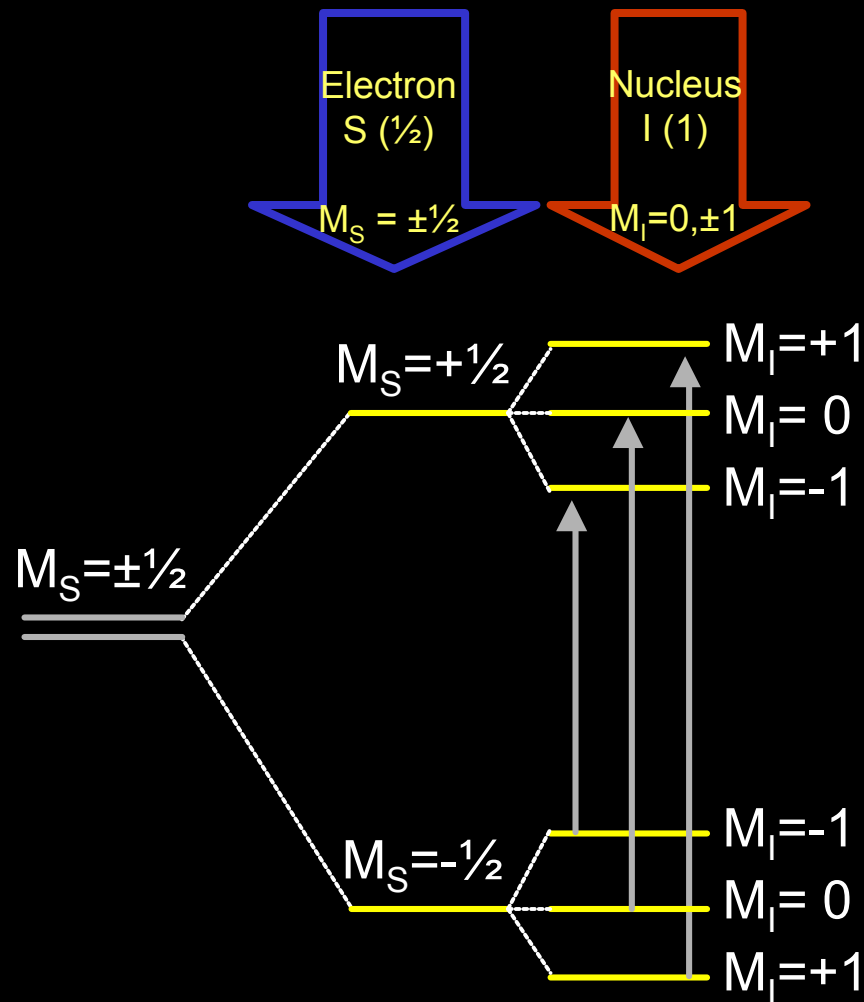
Hyperfine Coupling



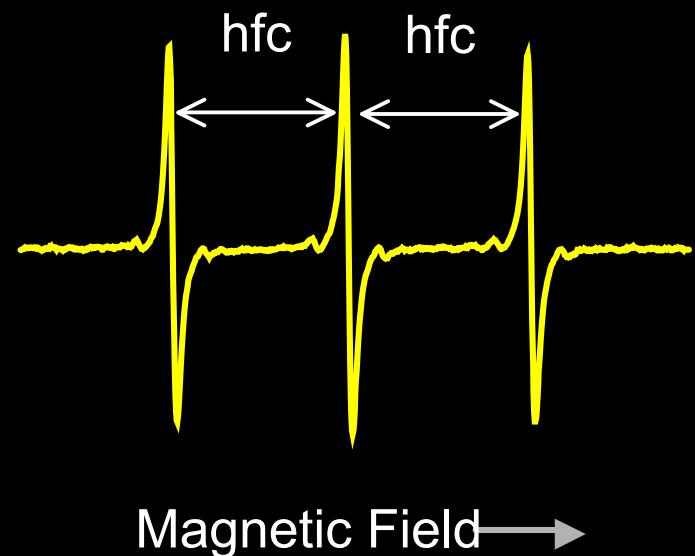
Selection Rule
 $\Delta M_S = \pm 1; \Delta M_I = 0$



Hyperfine Coupling



$S = 1/2;$
 $I = 1$
 Triplet



What do we do with EPR?

We can detect & measure free radicals and paramagnetic species

- High sensitivity (nanomolar concentrations)
- No background
- Definitive & quantitative

Direct detection

e.g.: semiquinones, nitroxides, trityls

Indirect detection

Spin-trapping

Species: superoxide, hydroxyl, alkyl, NO

Spin-traps: DMPO, PBN, DEPMPO, Fe-DTCs

Chemical modifications

Spin-formation : hydroxylamines (Dikhalov et al)

Spin-change : nitronyl nitroxides (Kalyanaraman et al)

Spin-loss : trityl radicals

Can we use EPR to measure free radicals from biological systems (*in vivo* or *ex vivo*)?

Yes! Intact tissues, organs or whole-body can be measured.
But there is a catch!

Biological samples contain large proportion of water. They are aqueous and highly dielectric. Conventional EPR spectrometers operate at X-band ((9-10 GHz) frequencies, which result in (i) 'non-resonant' absorption (heating) of energy and (ii) poor penetration of samples. Hence the frequency of the instrumentation needs to be reduced.

What is the optimum frequency? - depends on sample size

Frequency	~300 MHz	~750 MHz	1-2 GHz	~3 GHz	9-10 GHz
Penetration Depth	> 10 cm	6-8 cm	1-1.5 cm	1-3 mm	1 mm
Objects	Mouse, rat	Mouse	Mouse, rat heart	Mouse tail Topical (skin)	In vitro samples (~100 uL vol.)
Pioneers	Halpern et al Krishna et al	Zweier et al	Hyde et al Swartz et al Zweier et al	Hyde et al Zweier et al	

What else can we do with EPR?

We can use free radicals as “spying probes” to obtain information from biological systems

- A known free radical probes is infused or injected into the animal
- The change in the EPR line-shape profile, which is correlated to some physiological function, is then monitored as a function of time or any other parameter.
- The measurements can be performed in real-time and in vivo to obtain 'functional parameters'.

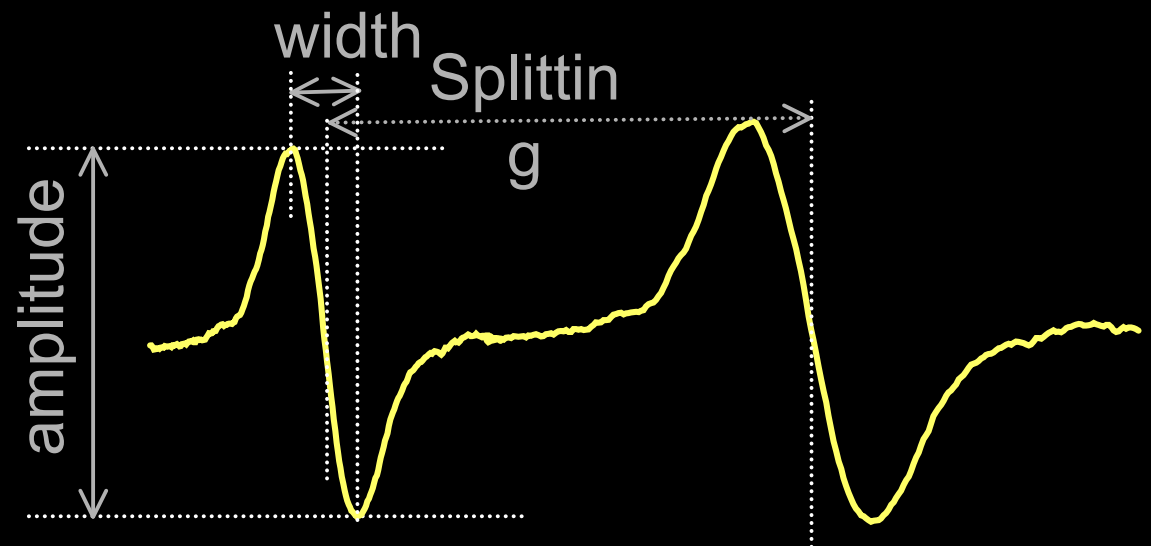
Functional parameters from an EPR spectrum

In vivo EPR spectroscopy is capable of providing useful physiologic and metabolic (functional) information from tissues

Oxygen, pO_2
Redox status
Acidosis, pH
Thiols (GSH)
Cell viability
Viscosity
Tissue perfusion
Molecular
motion

Redox status
Cell viability
Tissue
perfusion

Oxygen, pO_2
Acidosis, pH
Viscosity
Molecular
motion



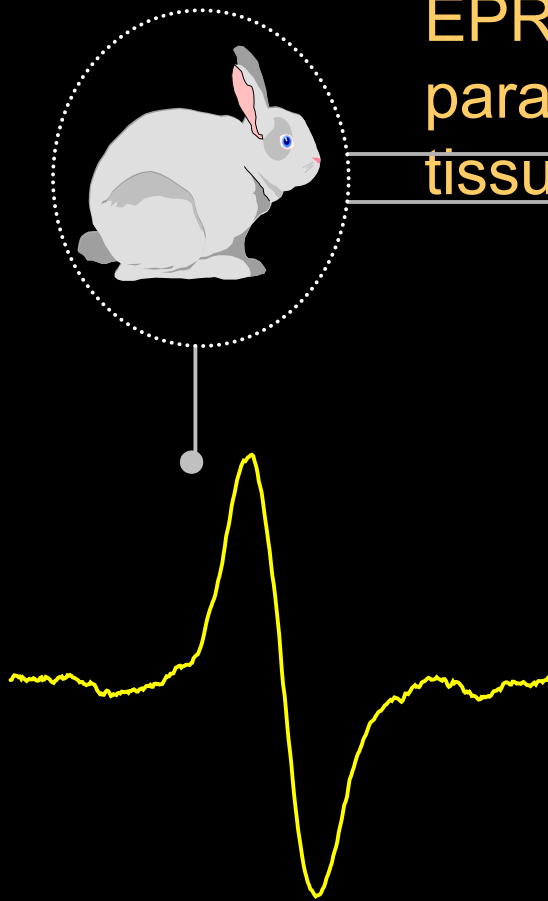
Can we image free radicals in biological systems?

Spatially-resolved information (mapping) can
be obtained using **EPR imaging (EPRI)**
techniques

Can we image free radicals in biological systems?

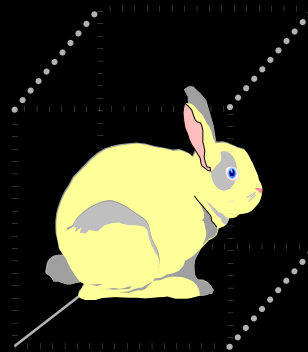
	<u>NMR</u>	<u>EPR</u>
Spin Probes radicals (endogenous)	Tissue protons (>50 M)	Free (\ll nM)
Probe Stability nanoseconds	Ideal	$<$
Relaxation time (LW) (LW: 1 G)	m sec	$< \mu$ sec
No suitable endogenous spin probes for EPRI image		Nothing to
Fast electronics needed for EPRI. image		No way to
(1989)		<i>Eaton & Eaton</i>

EPRI is capable of measuring the distribution of paramagnetic and free radical species in tissues



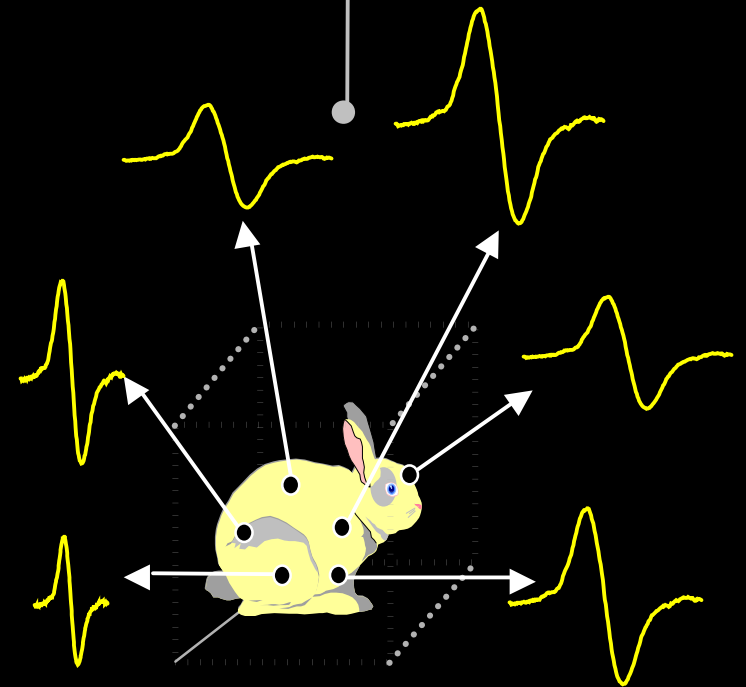
EPR Spectroscopy
Spatially-unresolved

0 + 1 dimensional



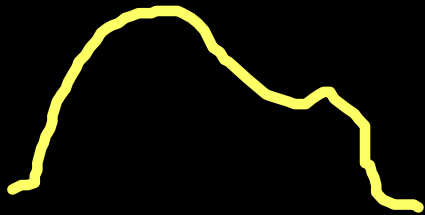
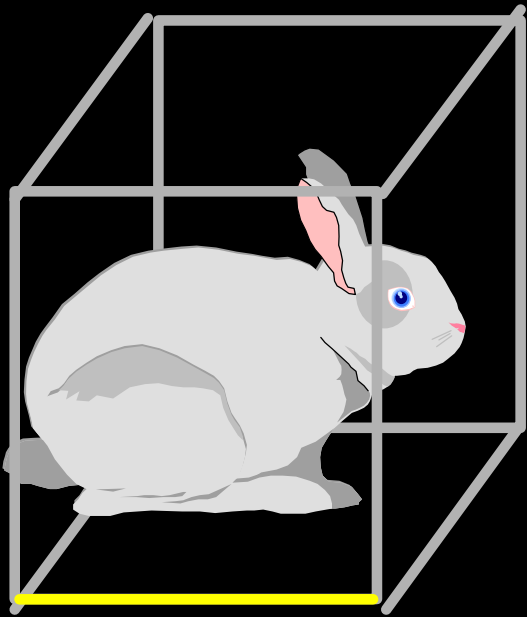
Spatial Imaging
Spatially-resolved
Spin density

3 + 0 dimensional

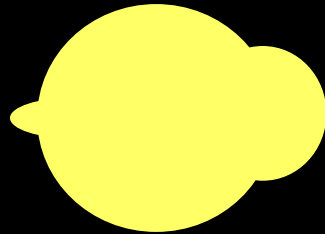
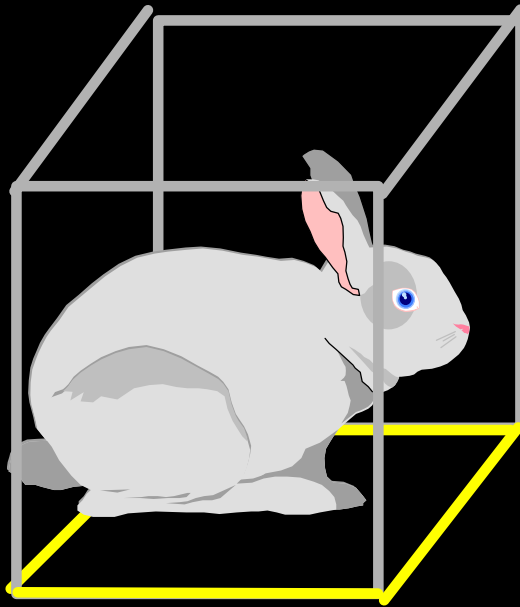


Spectral-spatial Imaging
Spatially-resolved
Spectral shape

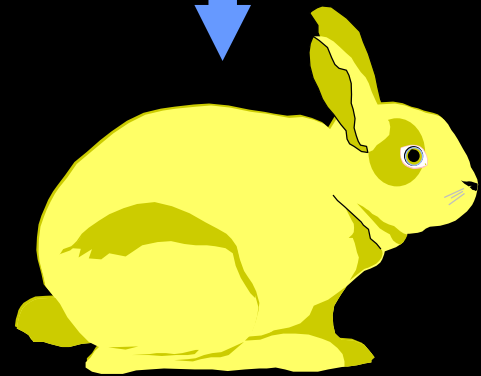
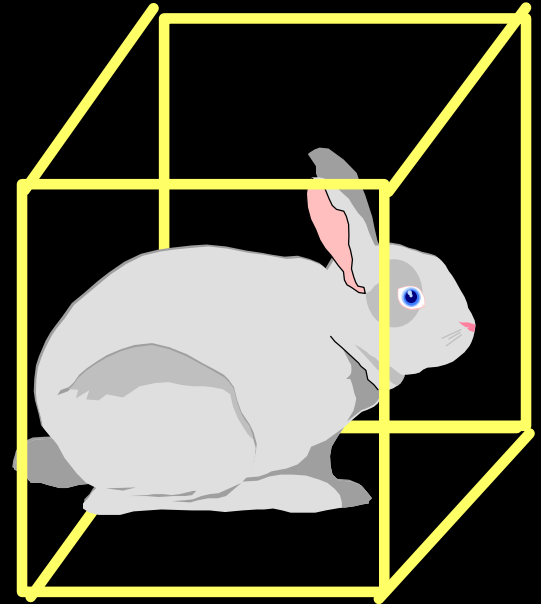
3 + 1 dimensional



1D SPATIAL



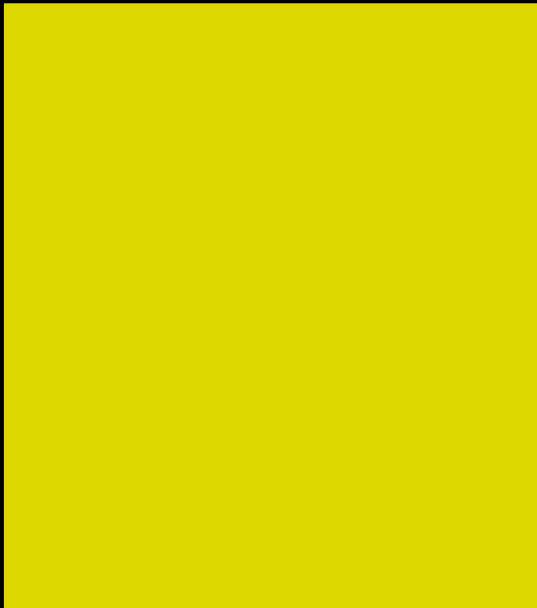
2D SPATIAL



3D SPATIAL

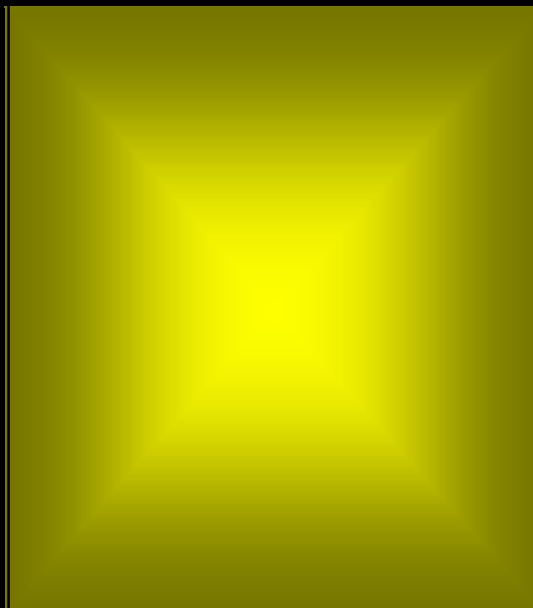
Gradient Magnetic Field

Homogeneous
(Spectroscopy)



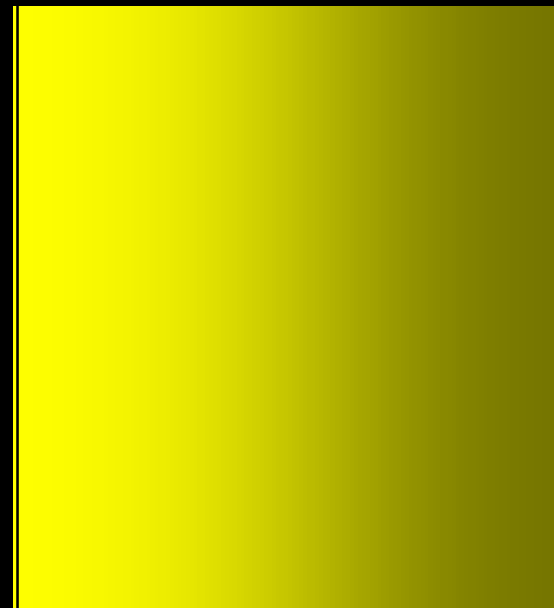
Distance --->

Inhomogeneous
(Not useful)



Distance --->

Gradient
(Imaging)

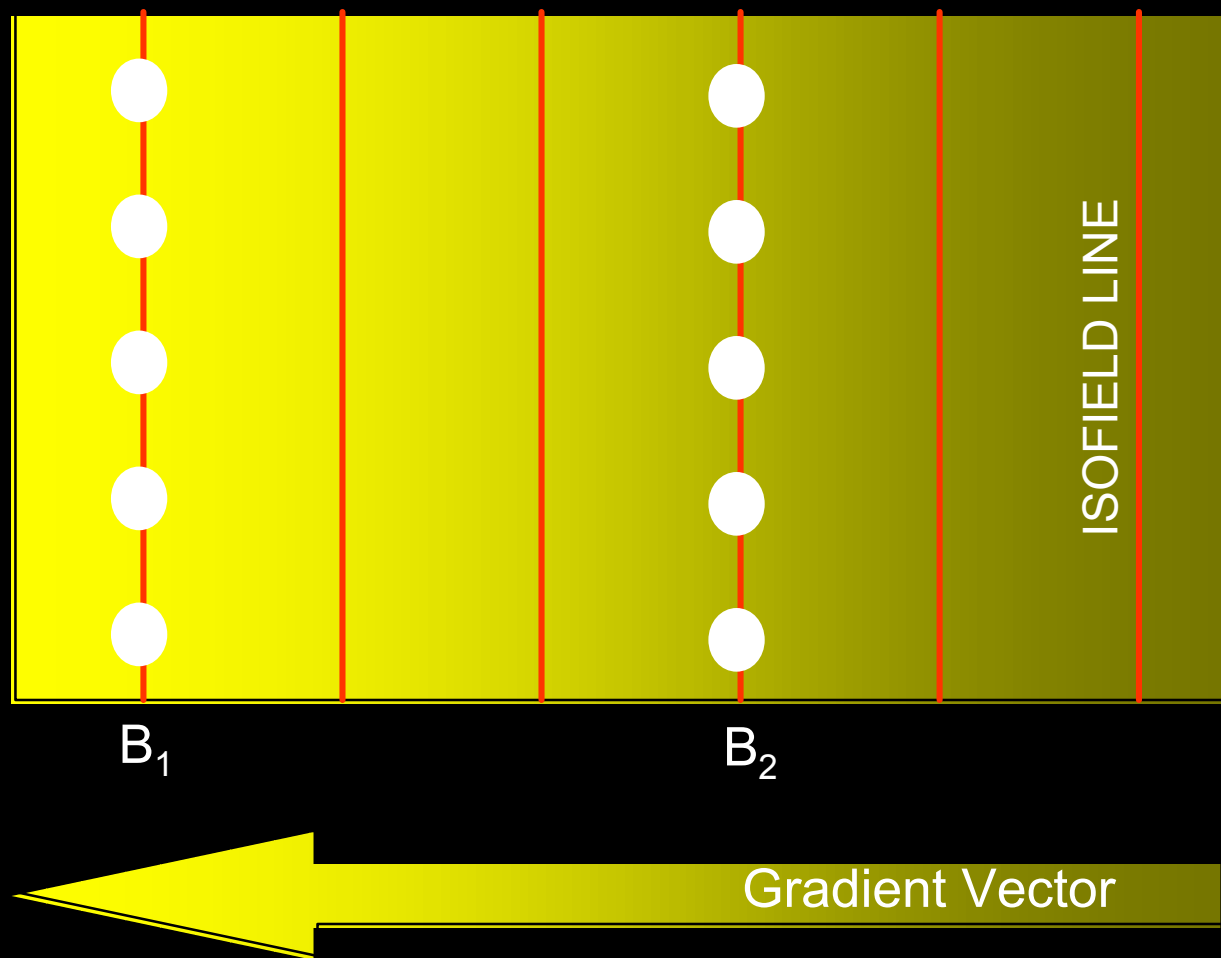


Distance --->



<----- Magnetic Field

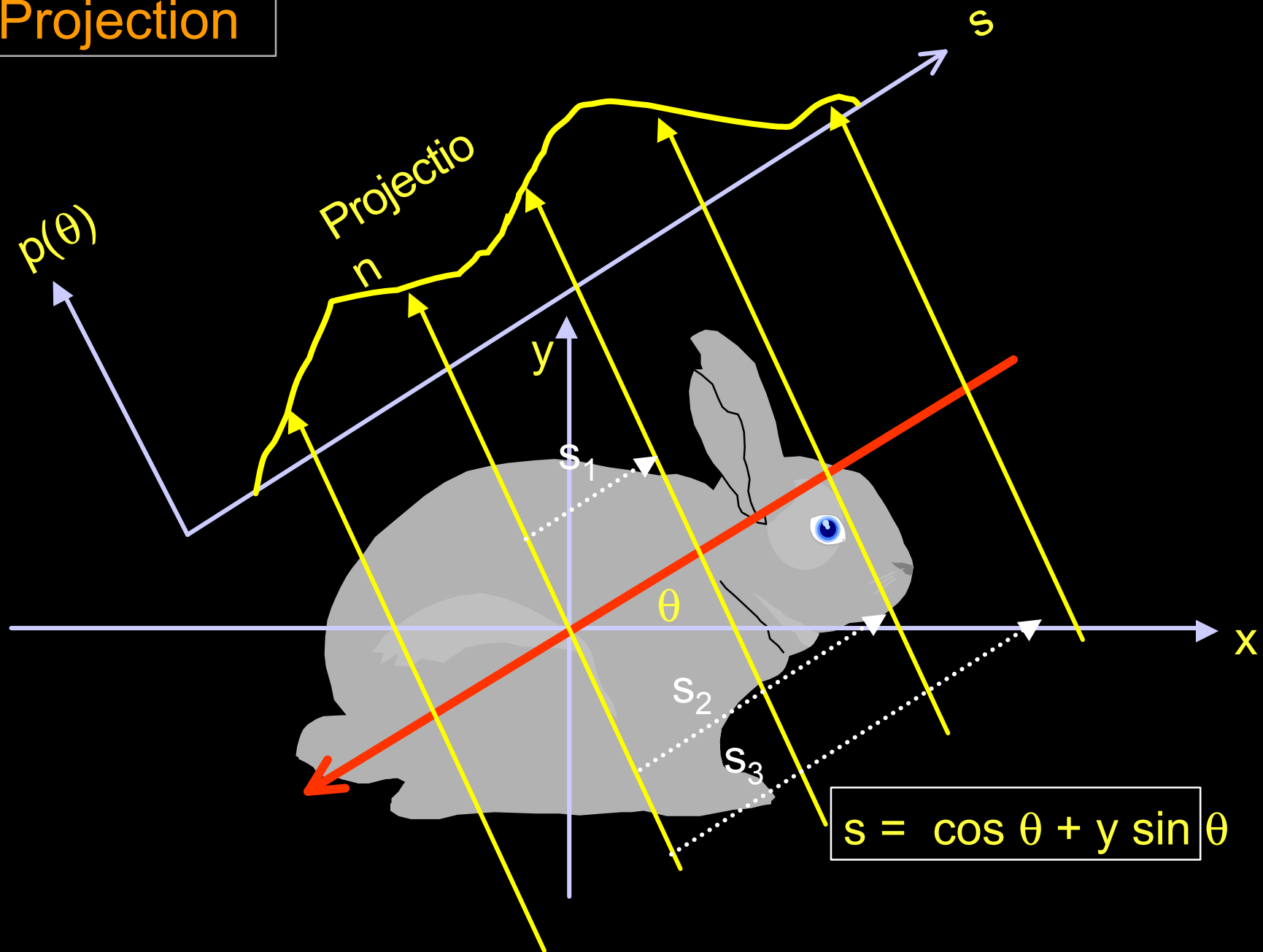
Gradient Magnetic Field



$$B_1 > B_2$$

In the conventional CW EPR sweep mode, spins at B_1 will come into resonance first.

Projection



Projection Acquisition

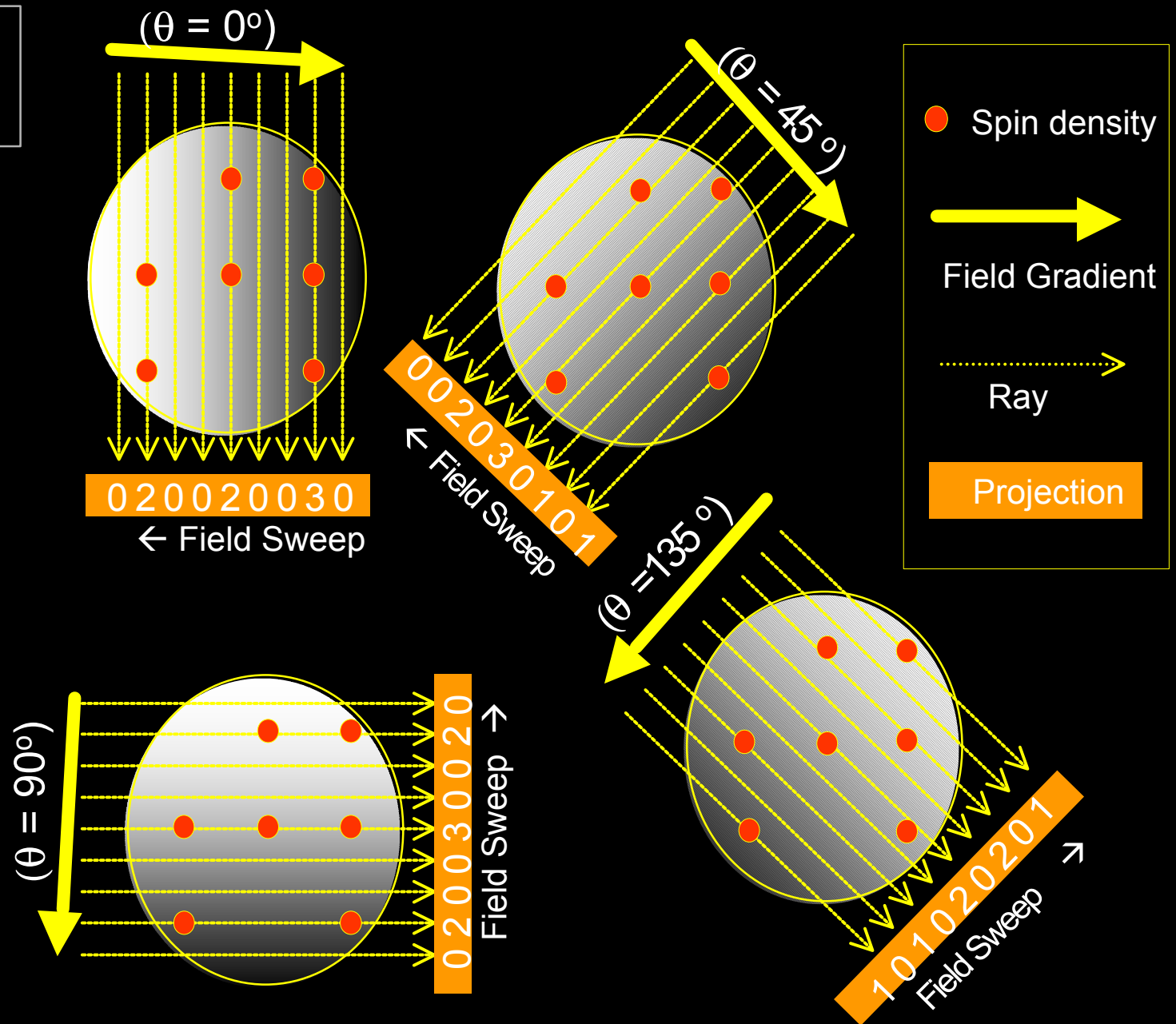
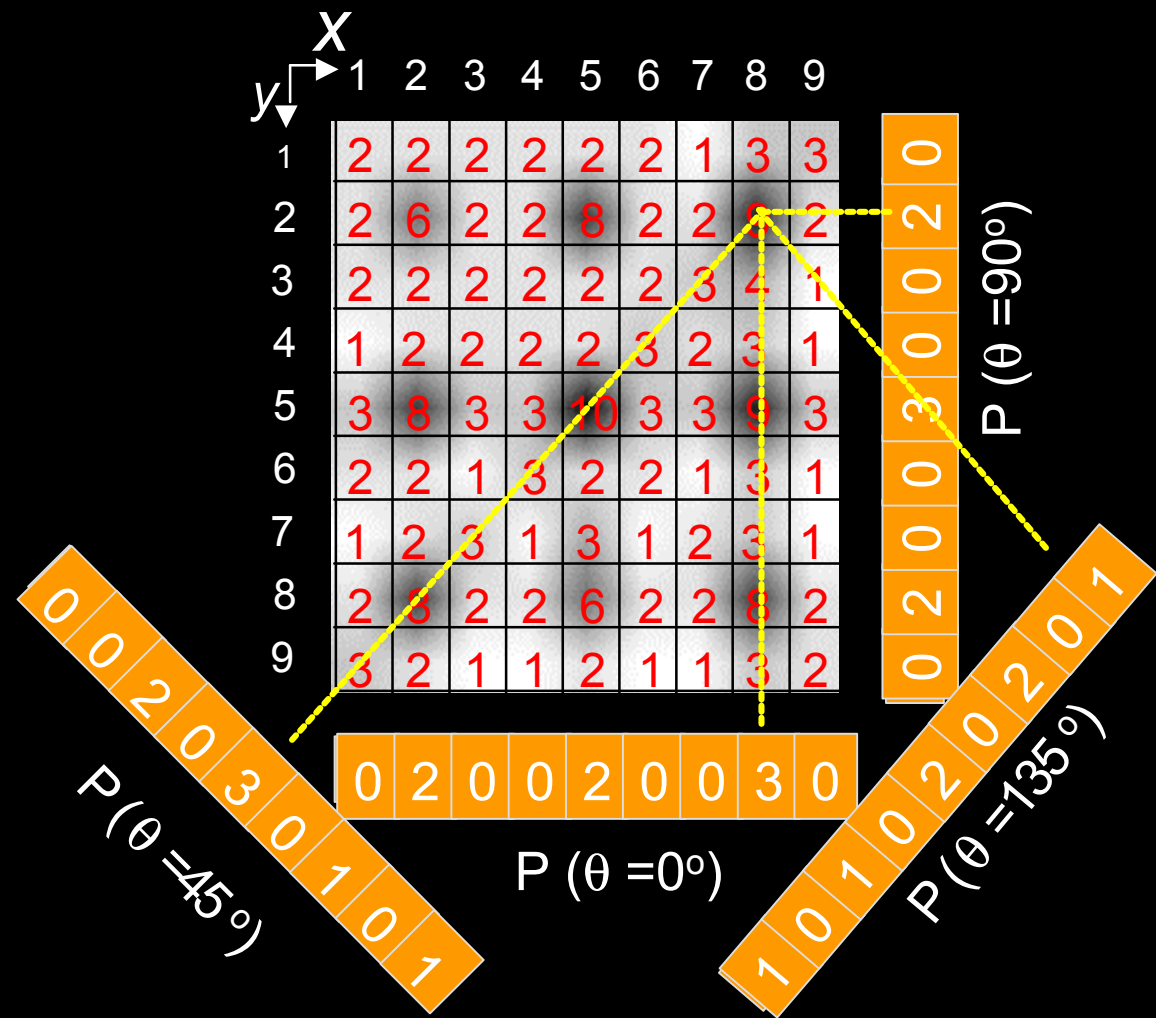
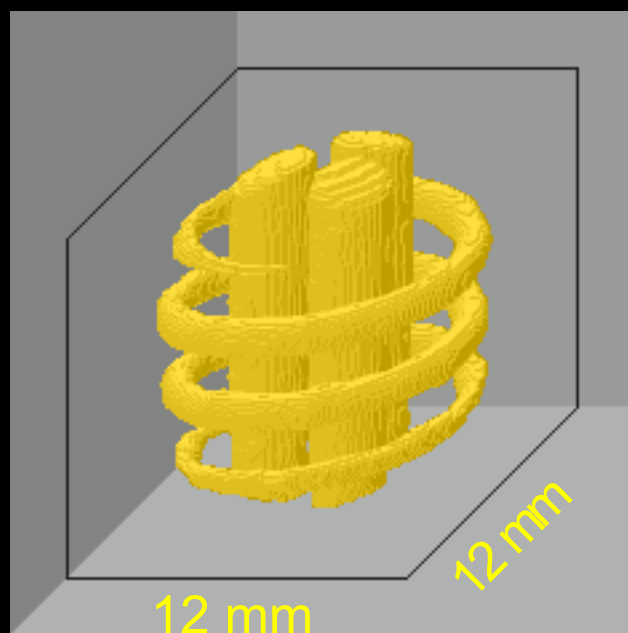


Image Reconstruction by Backprojection



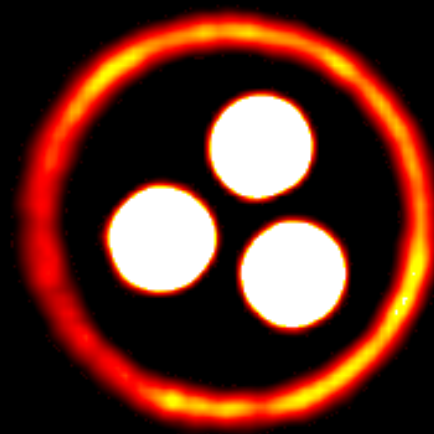
3D IMAGING OF A SPIRAL PHANTOM

A pack of three identical tubes (i.d.: 3 mm) and a polyethylene tubing (id: 1.1 mm) wound around the pack. The tubes were filled with 0.5 mM solution of TAM.



0 256

3D composite view



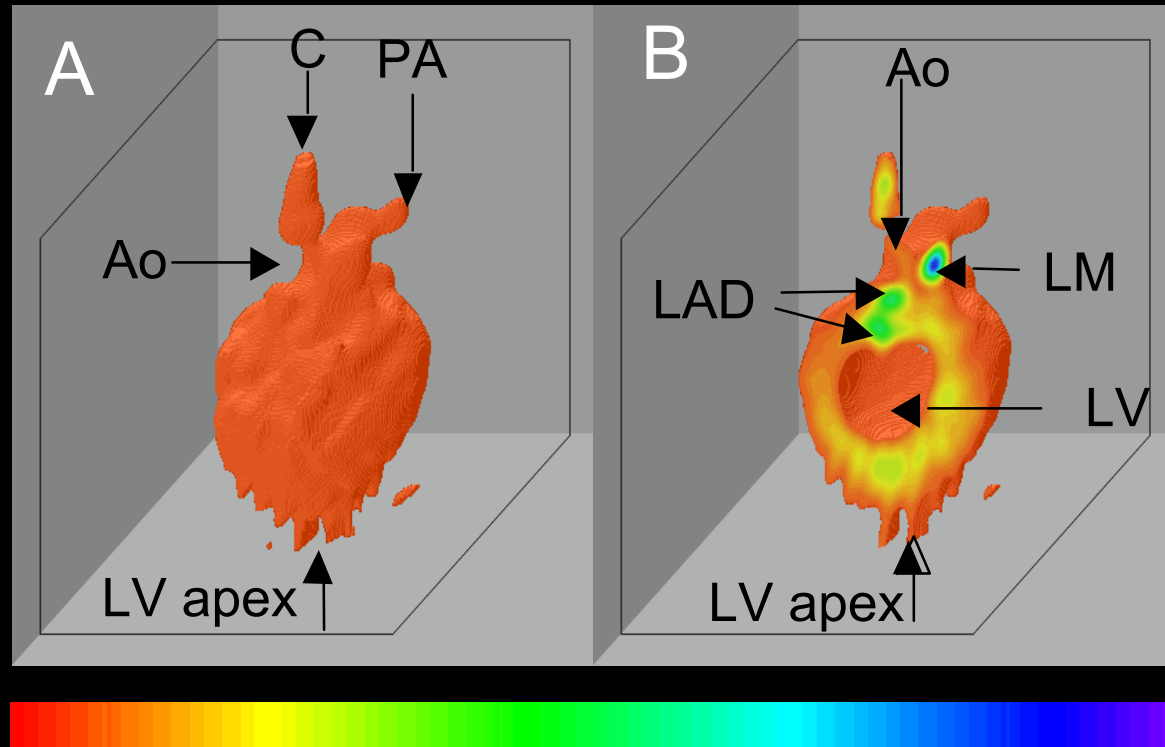
12 mm

0 256

A 2D projection of the
image

Proj., 1024; gradient, 10 G/cm; acq. time, 51.6 min; resolution, 100 μ m.

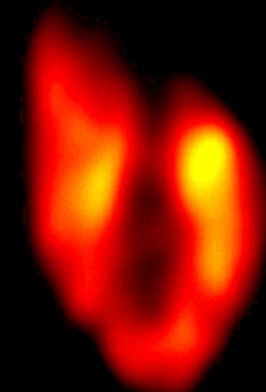
3D Image of a rat heart perfused with glucose char



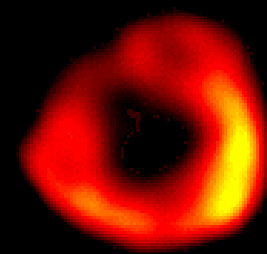
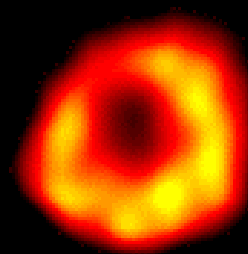
3D EPR image of an ischemic rat heart infused with glucose char suspension oximetry label. **A:** Full view **B:** A longitudinal cutout showing the internal structure of the heart. Ao, aortic root; C, cannula; PA, pulmonary artery; LM, left main coronary artery; LAD, left anterior descending artery; LV, left ventricular cavity.

Gated Imaging of Rat Heart

Transverse slices



Longitudinal slices



systolic

diastolic

IMAGING OF RAT KIDNEY PERFUSED WITH TAM

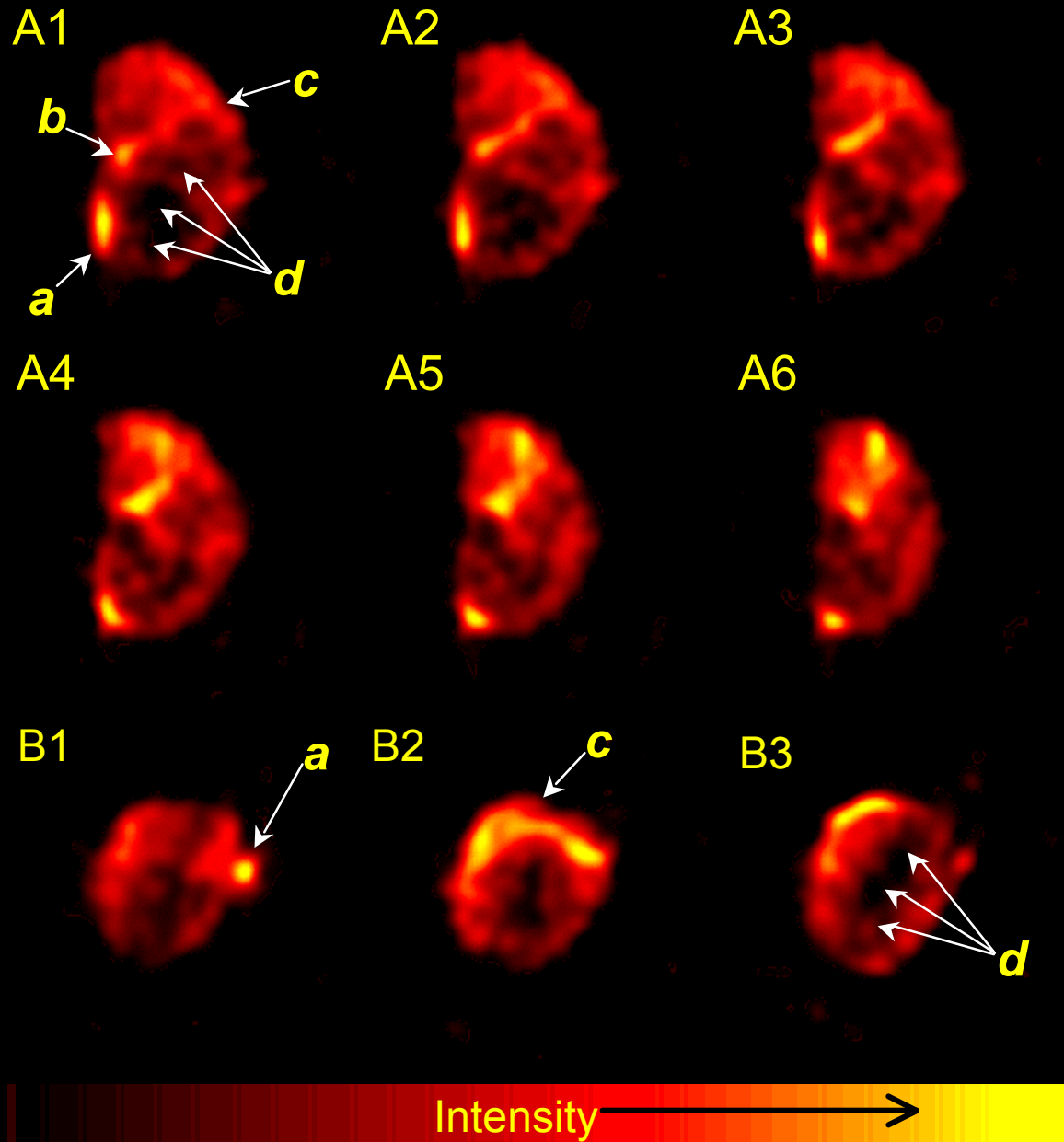
Representative slices
(24x24 mm²,
thickness, 0.19 mm)
obtained from a 3D
spatial image.

A1-A6: Vertical slices
B1-B3: Transverse
slices

a - cannula
b - renal artery
c - cortex

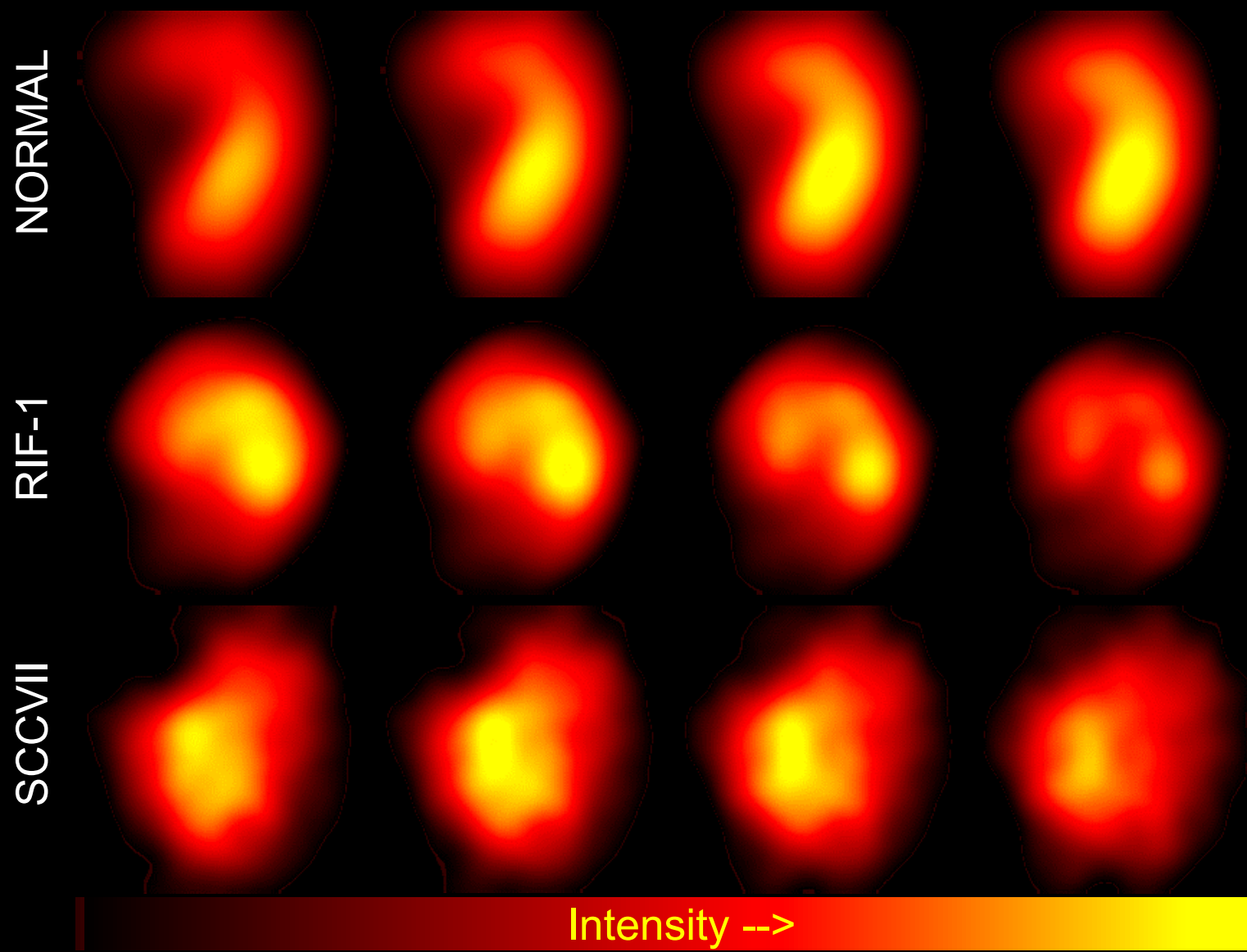
d - papilla

Proton, 1024
grad, 25.0 G/cm;
acq. time, 76.8 min;
resolution, 200 μ m



3D IMAGING OF NITROXIDE DISTRIBUTION IN TUMORS

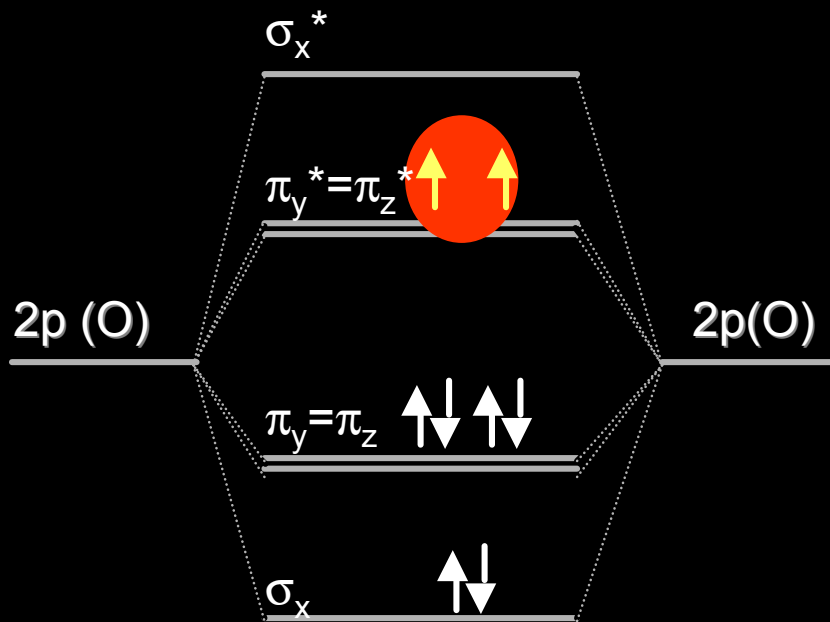
SLICES (0.3 MM) FROM 3D IMAGES OF MURINE TUMORS (3-CP; 100 mg/kg)



C3H mice; gradient 20 G/cm; 144
projections; 10x10 mm²

Kuppusamy, P., et al. Cancer Research, 58, 1562-1568
(1998)

Molecular oxygen is paramagnetic



Molecular oxygen has two unpaired electrons

- Oxygen gives strong EPR signals in the gas phase
- However, no EPR spectrum has been reported for oxygen dissolved in fluids. (too broad!)
- Thus, there seems to be no possibility for direct detection of oxygen in biological systems using EPR
- However, molecular oxygen can be measured and quantified indirectly using **spin-label EPR oximetry**

EPR oximetry probes

Particulate (Solid) probes

Lithium phthalocyanine (LiPc)
Sugar chars
Fusinite
Coal
India ink

What is reported?

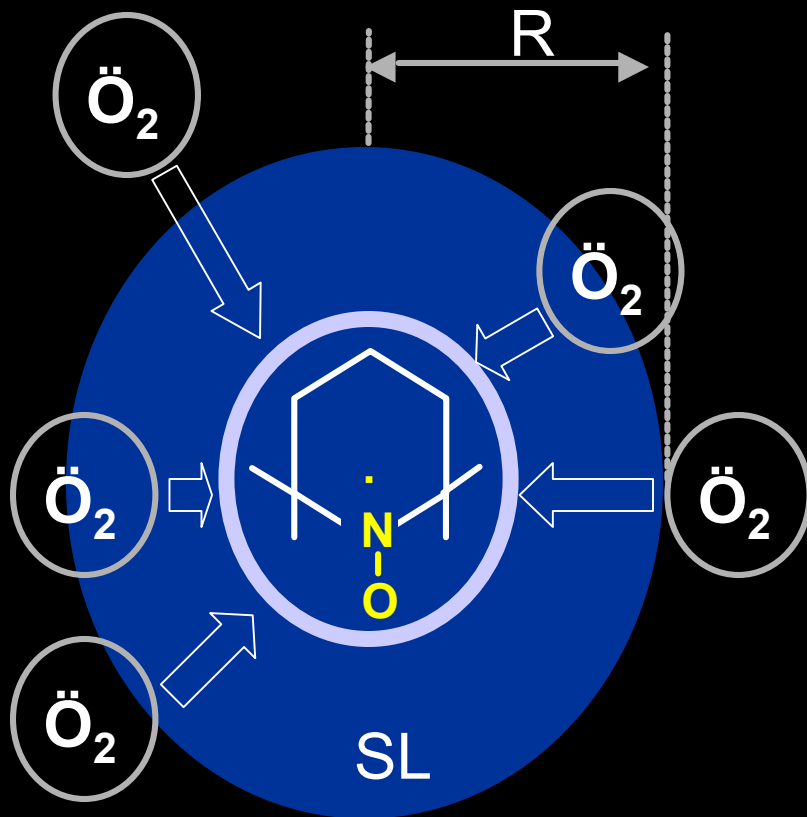
- pO_2 (mmHg/Torr)
- Localized Measurement
- Resolution < 0.2 mmHg
- Repeated Measurements
- Stable for days to weeks
- Independent of medium

Soluble probes

Nitroxides
Trityl radicals

- Concentration (μM) of dissolved oxygen in the bulk volume
- Resolution 2-10 mmHg

Principle of EPR oximetry



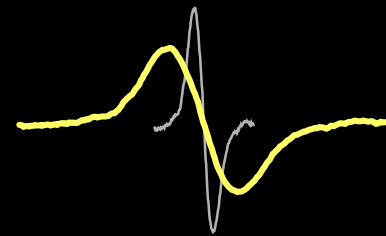
Bimolecular collision between SL and oxygen leads to Heisenberg spin exchange

The collision frequency ω , according to the hard sphere theory of Smoluchowski is

$$\omega = 4\pi R\rho(D_{SL} + D_{O_2}) [O_2]$$

which translates to EPR line-broadening as

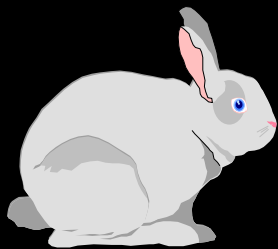
$$\Delta w = k D_{O_2} [O_2]$$



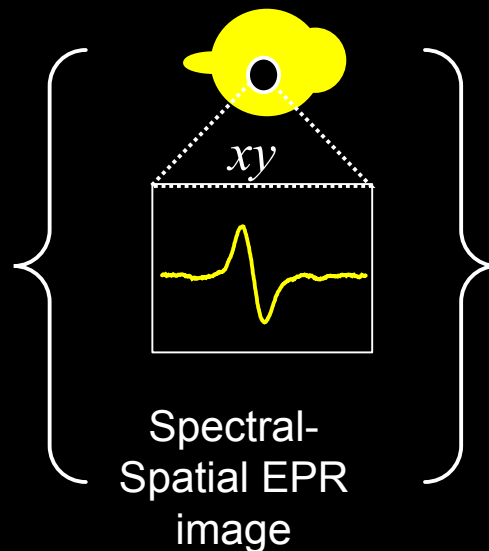
Mapping of Oxygen

Mapping of oxygen in biological tissues is possible by spectral-spatial or 'spectroscopic' EPR imaging.

Object

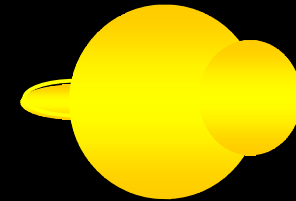


Data



Spin density

Information



e.g. Oxygen

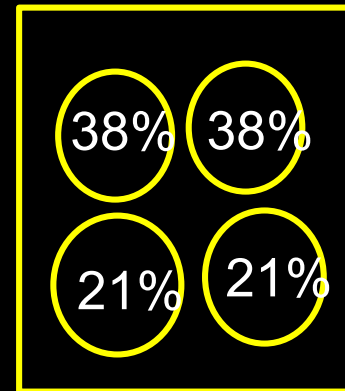
EPR Oxygen Mapping (EPRoM)

Phantom
of tubes with
 ^{15}N -PDT

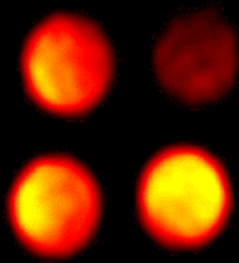
[PDT, mM]



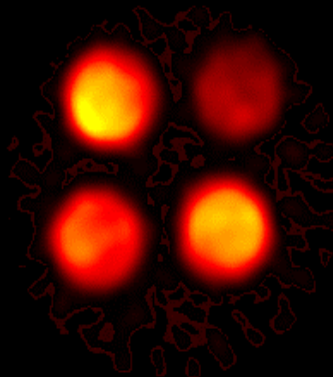
[Oxygen]



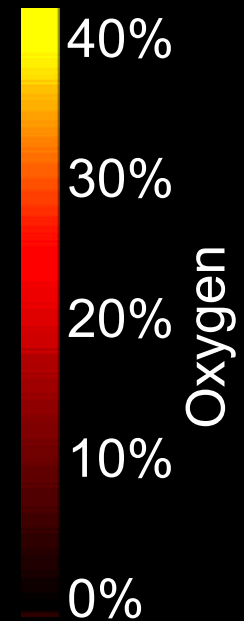
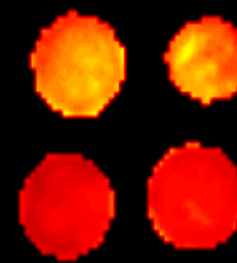
Amplitude Map



Spin Density Map

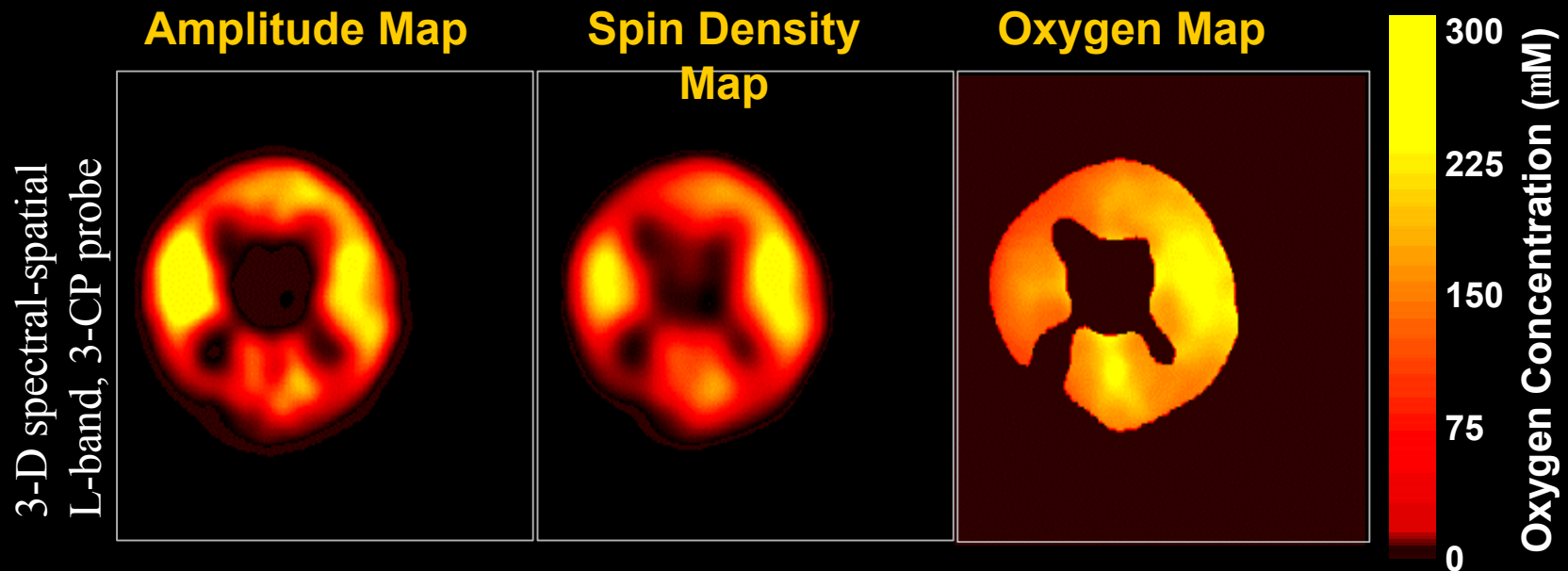
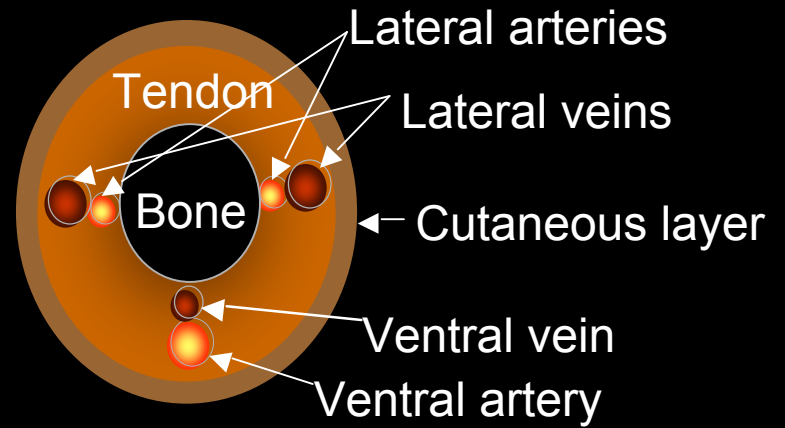
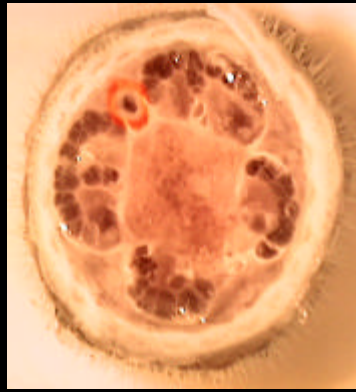


Oxygen Map



S. Sendhil Velan, R. G. S. Spencer, J. L. Zweier & P. Kuppusamy, Magn. Reson. Med. 43, 804-809 (2000)

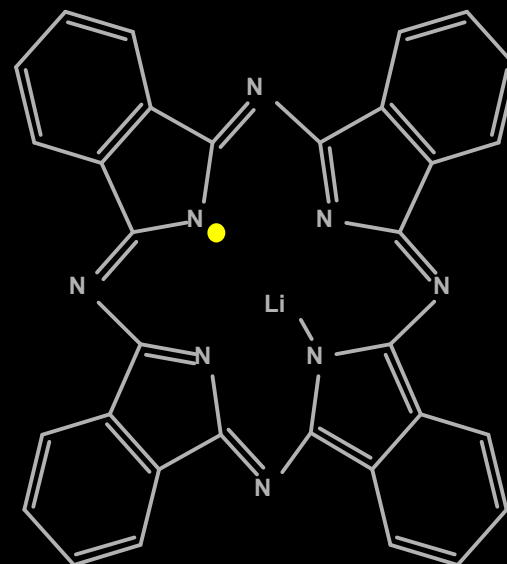
Mapping of arterio-venous oxygenation in a rat tail, *in vivo*



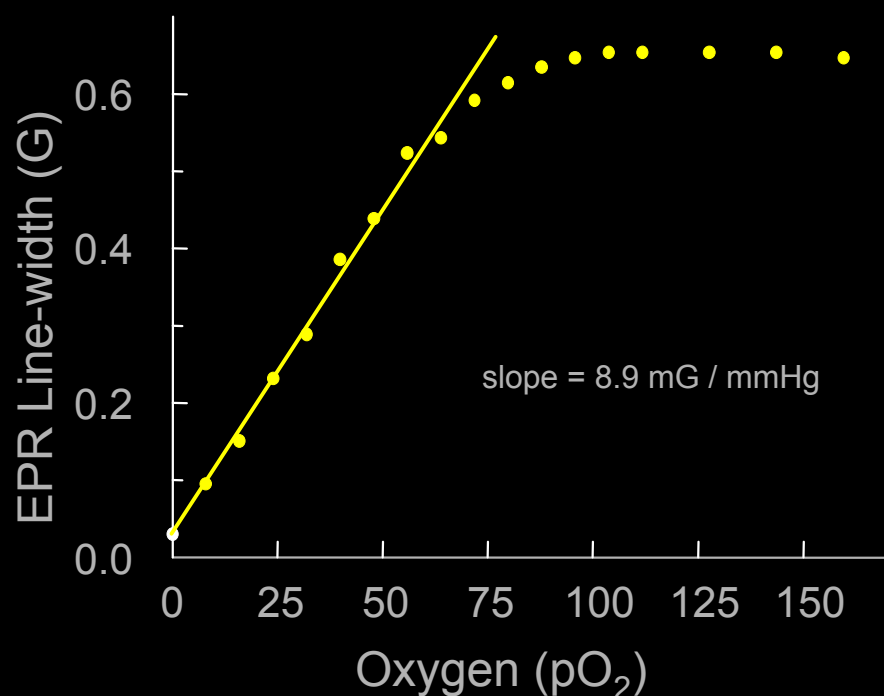
LiPc (Lithium

Phthalocyanine)

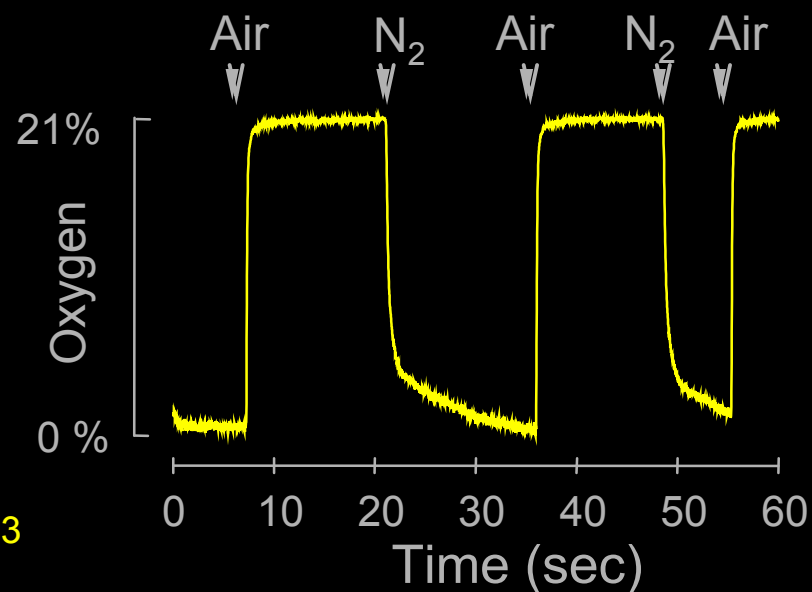
Oxygen sensitive (T_2) EPR probe



Response to Oxygen

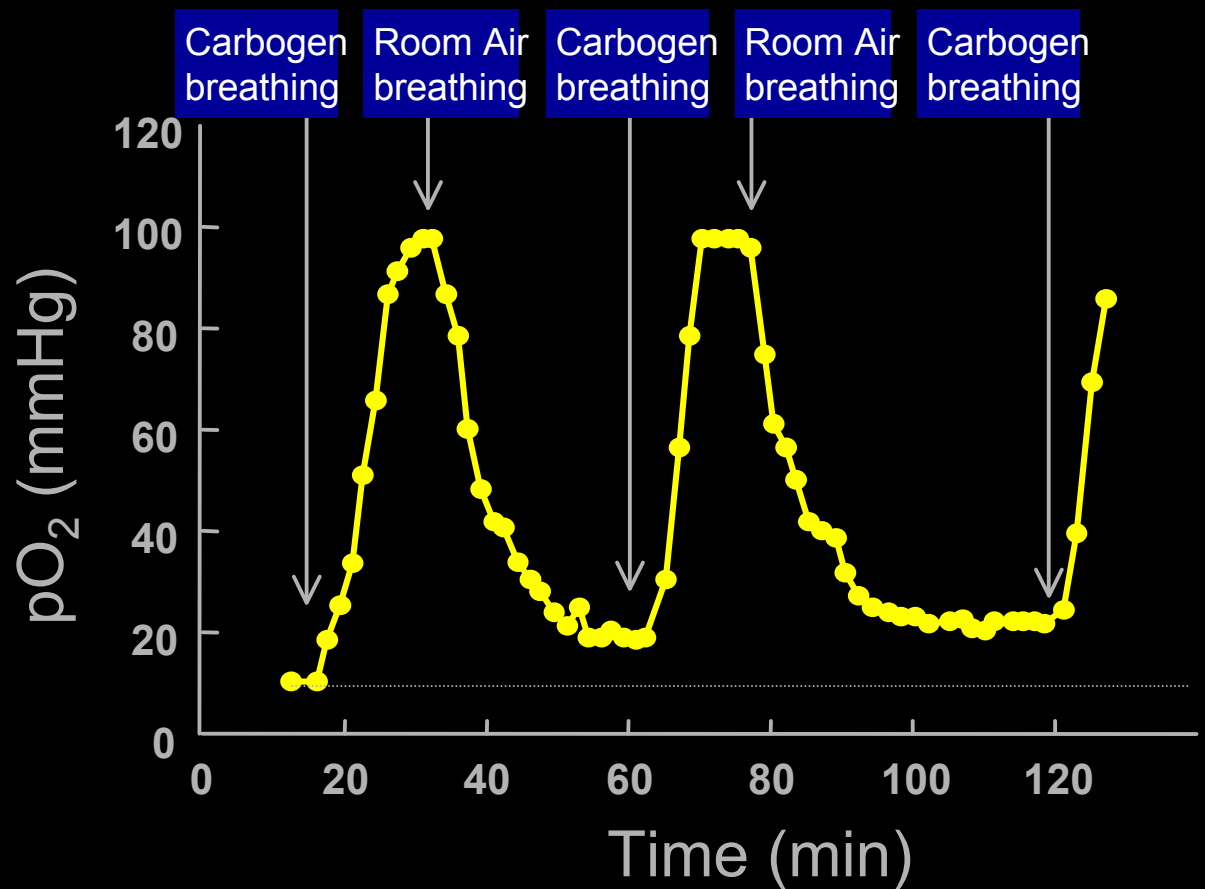
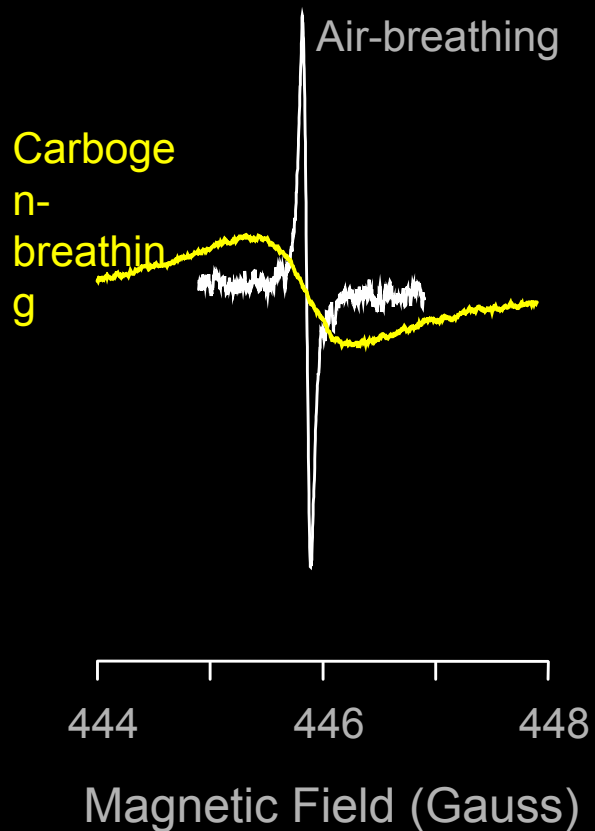


Oxygen Time Response



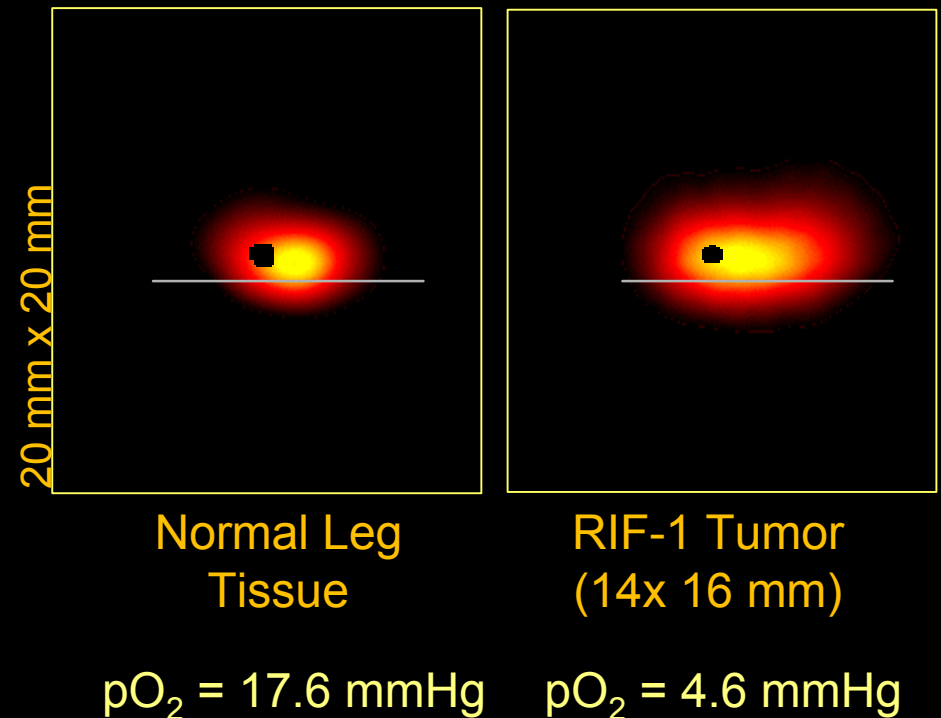
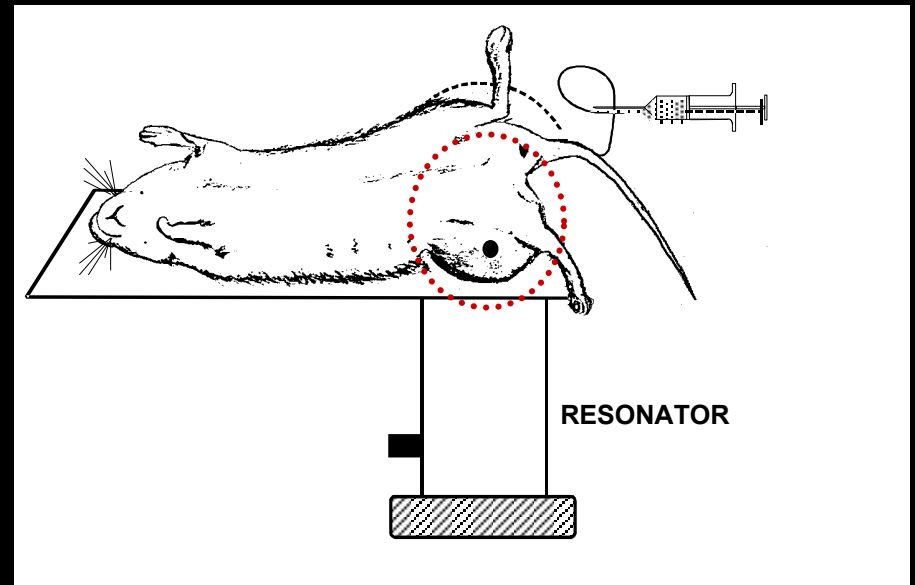
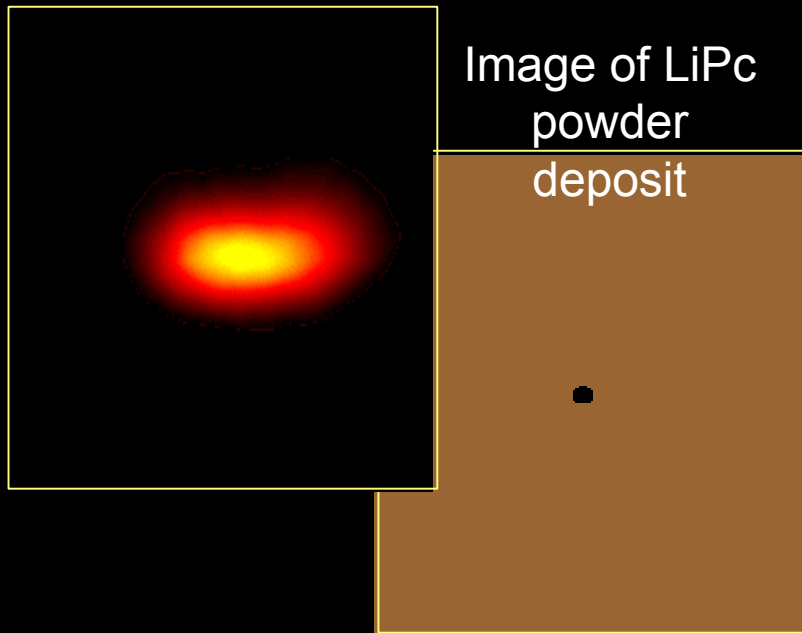
Ilangovan, G., Li, H., Zweier, J.L., Kuppusamy, P.
J. Phys. Chem. B 104, 4047 (2000); 104, 9404 (2000); 105, 5323 (2001)

Oxygenation of RIF-1 Tumor (Carbogen-breathing)

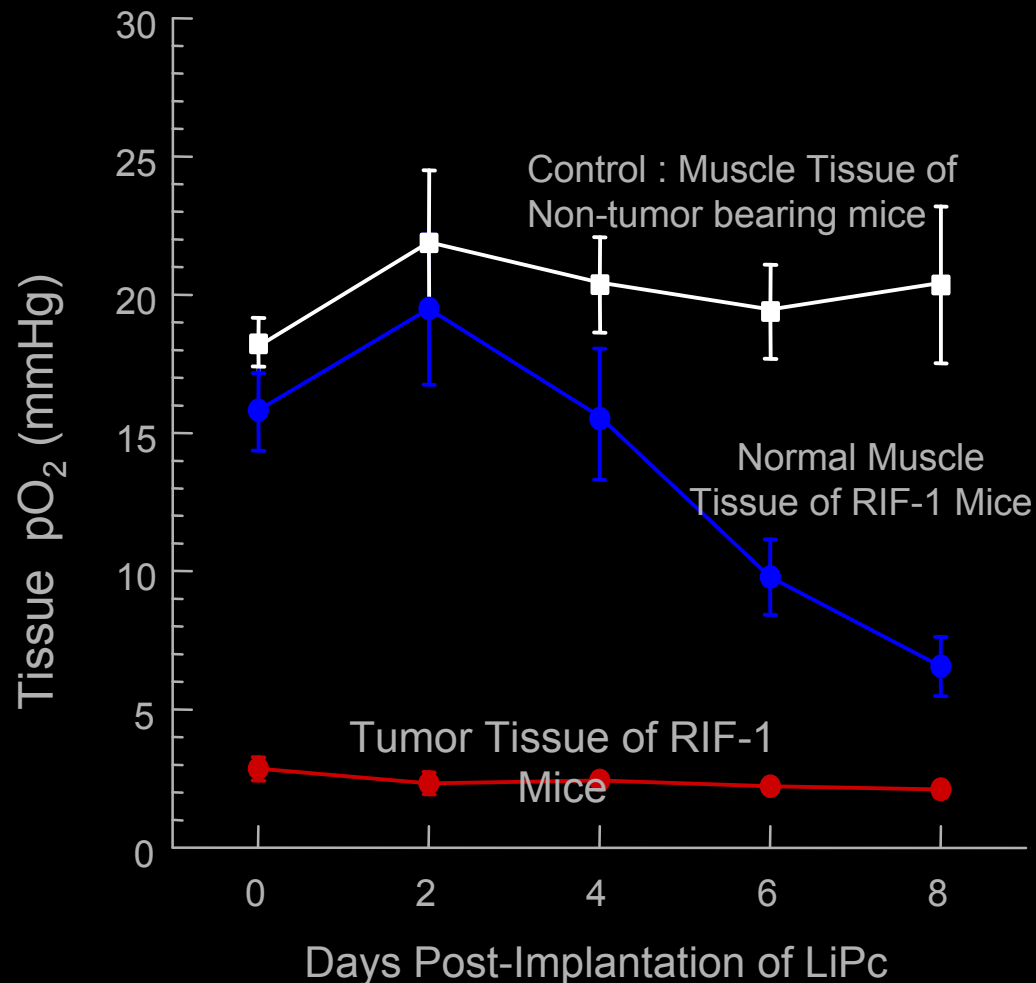


Oxygen Measurements using LiPc, a Particulate EPR Probe

Co-imaging of the
oximetry probe in the
tumor tissue
Perfusion image
of a nitroxide



In vivo measurements of pO_2 from tumor and normal gastrocnemius muscle tissues of RIF-1 tumor-bearing mice.

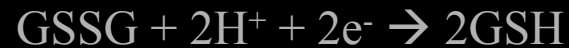


LiPc particles were implanted in the tumor on the right leg and normal muscle on the left leg and tissue pO_2 values were repeatedly measured on the same animals for up to 8 days using EPR oximetry. (N = 5)

Redox Status

Redox State describe the ratio of the interconvertible oxidized and reduced form of a specific redox couple

GSSG/2GSH



$$E_{\text{hc}} = E_0 - (RT/nF) \log([\text{GSH}]^2/[\text{GSSG}])$$

Redox State = Reduction potential \times concentration

Redox Status applies to a set of redox couples.
It is the summation of the products of the reduction potential and reducing capacity of **all the redox couples** present

GSSG/2GSH

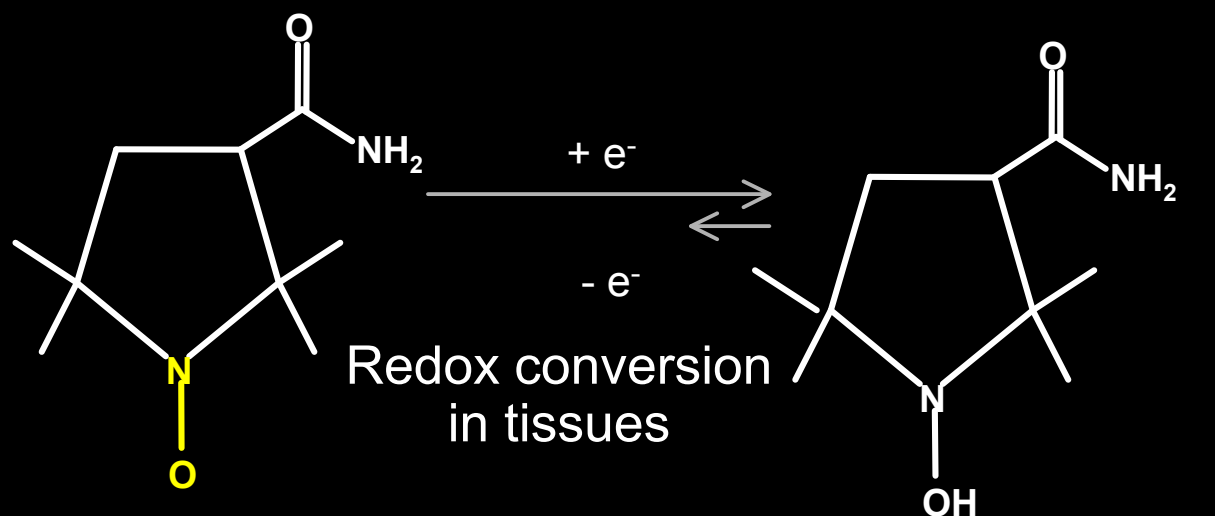
NADP⁺/NADPH

TrxSS/Trx(SH)₂

$$\text{Redox Status} = \sum [\text{Reduction potential} \times \text{concentration}]_i$$

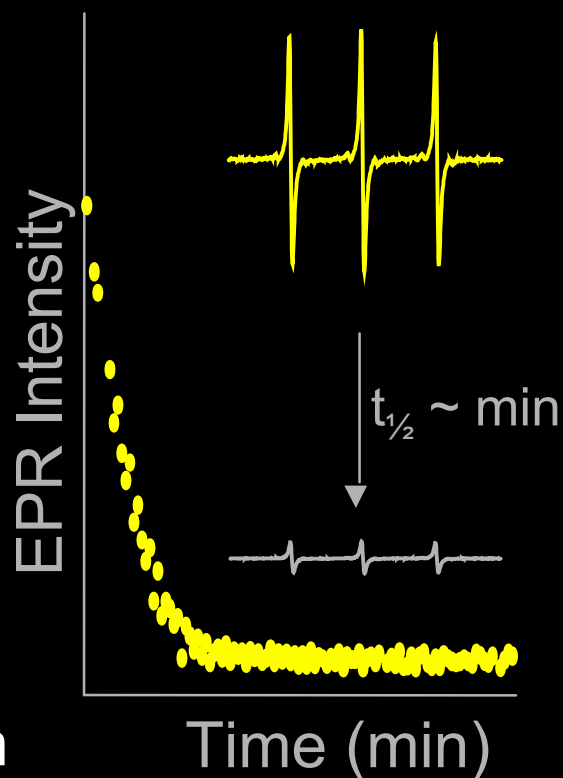
Schaefer, F. Q. & Buettner, G. R. Redox environment of the cell as viewed through the redox state of the glutathione disulfide/glutathione couple. Free Radic. Biol. Med. 30, 1191-1212 (2001)

Nitroxides as probes of tissue redox status



Nitroxide
EPR 'active'

Hydroxylamin
EPR 'inactive'

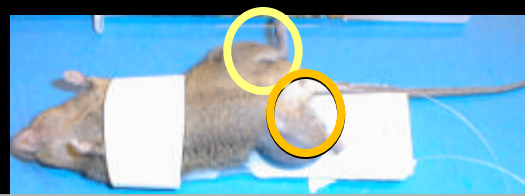


Swartz et al, Free Radic. Res. Commun., 9, 399-405
(1990)

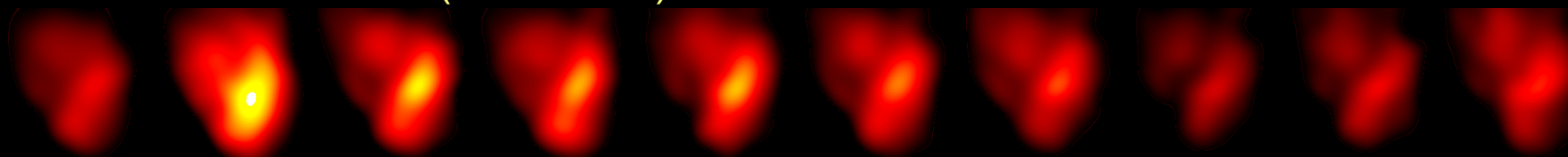
Kuppusamy et al, Cancer Research, 58, 1562-1568
(1998)

Krishna et al, Breast Disease, 10, 209-220 (1998)

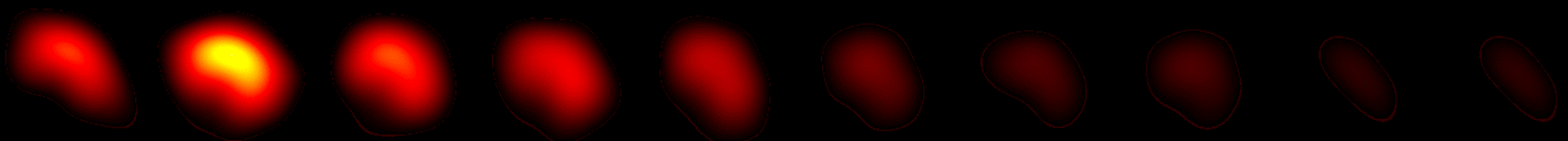
Reduction of 3-CP in the Normal & Tumor Tissue



NORMAL TISSUE (LEFT LEG)



RIF-1 TUMOR (RIGHT LEG)



3.0 4.5 6.0 7.5 9.0 10.5 12.0 13.5 15.0 16.5

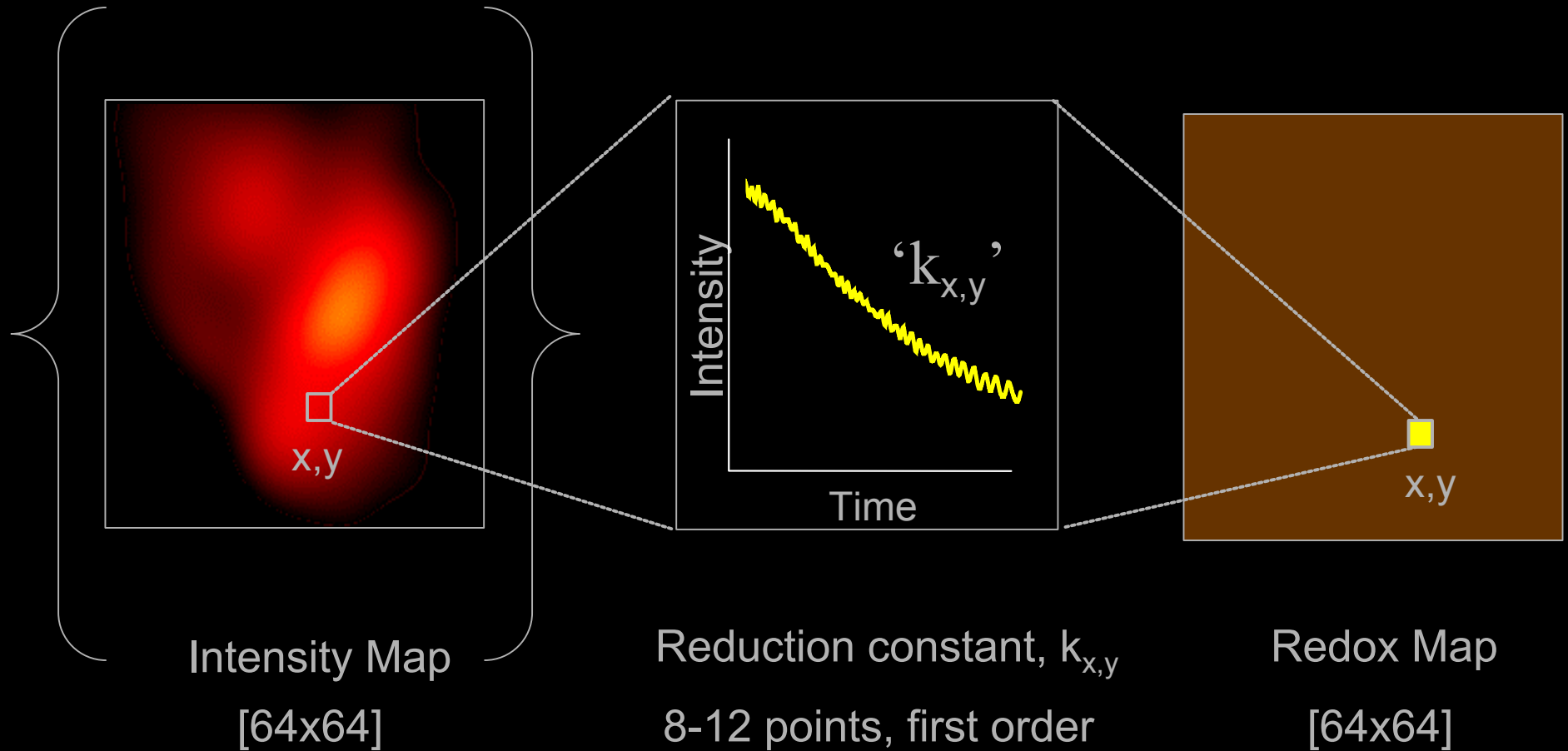
Time (min)

Intensity -->

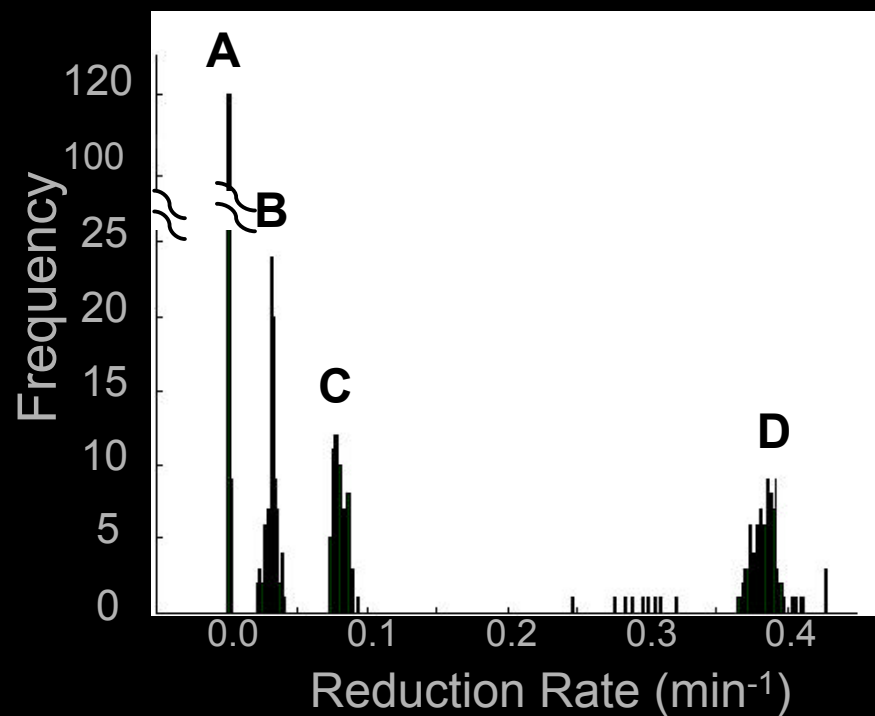
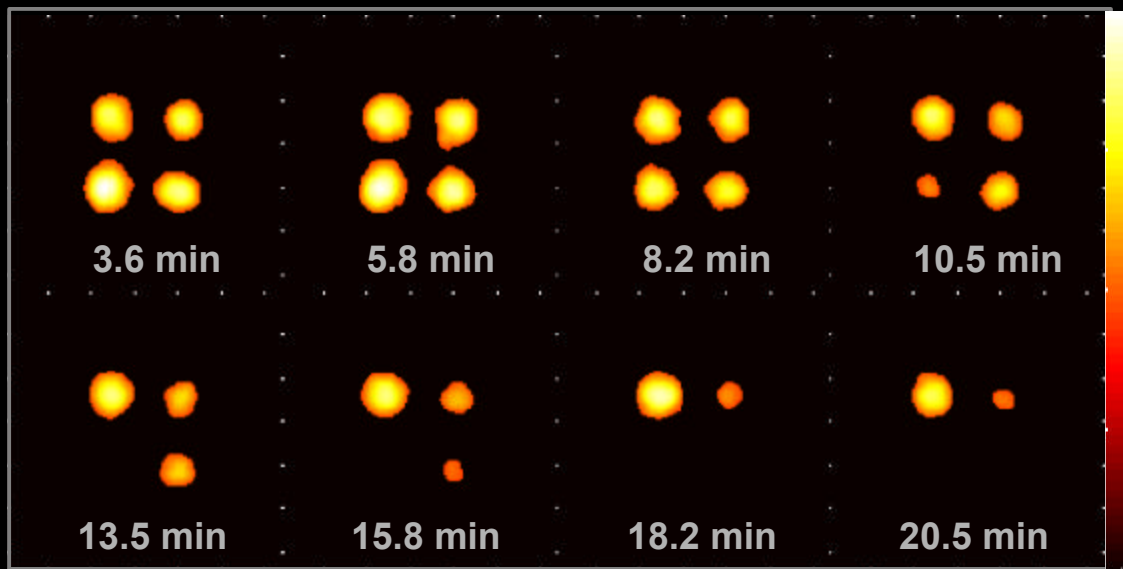
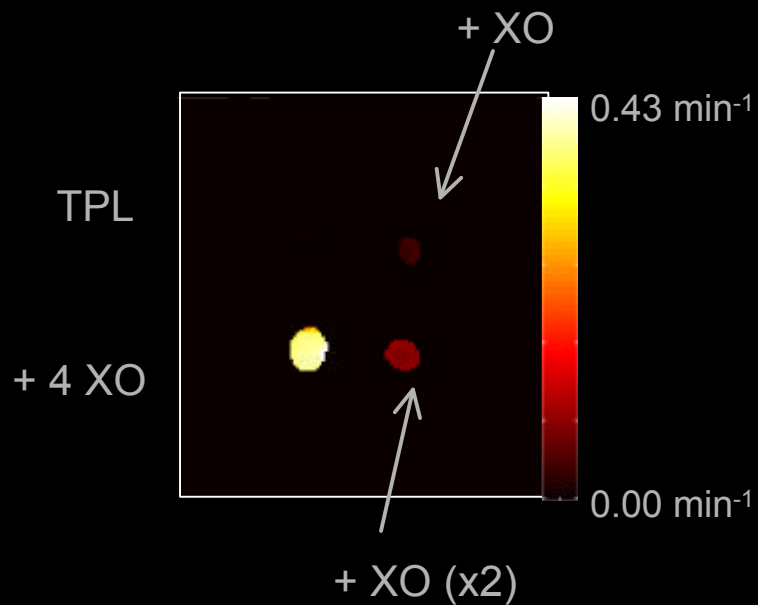
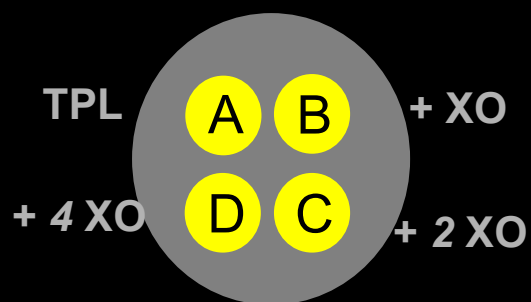
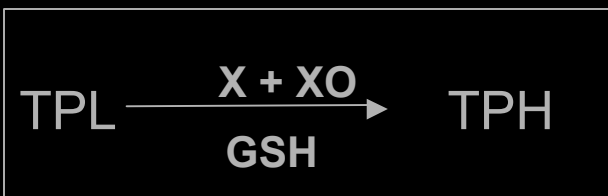
C3H mice with RIF-1 tumor; ~30 g bw; dose: 100 mg/kg, iv; Measured *in vivo* using surface resonator at L-band (1.25 GHz); Images: 10x10 mm²

Kuppusamy, P., et al. Cancer Research, 58, 1562-1568 (1998).

Reconstruction of Tissue 'Redox Status' Image

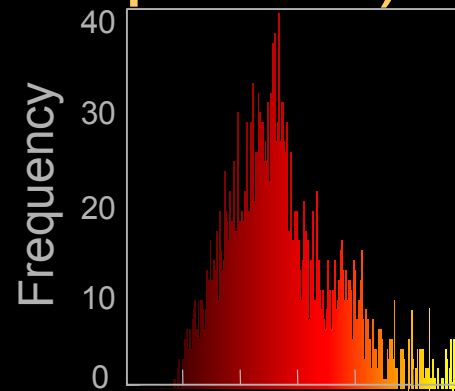
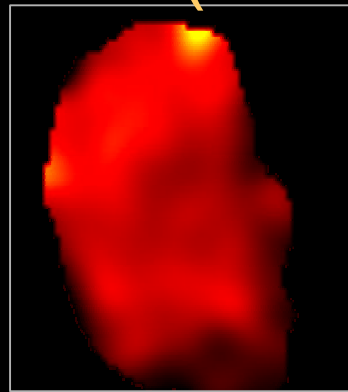


REDOX MAPPING BY EPR IMAGING (VALIDATION EXPERIMENT)



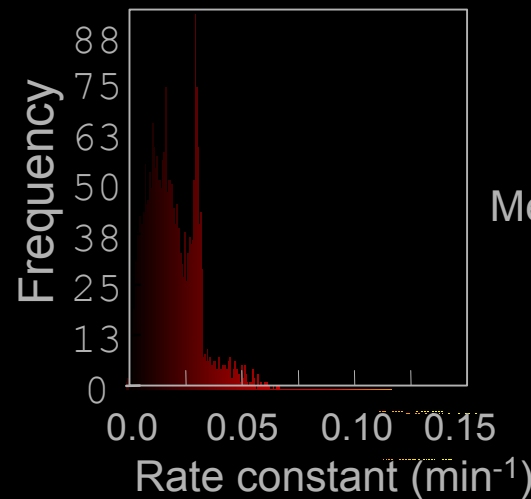
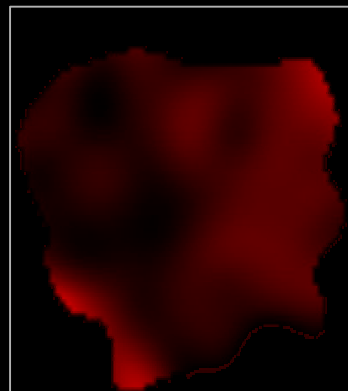
Redox Mapping of Tumor: Effect of BSO (GSH Depletion)

RIF-1



Median: 0.054 min⁻¹

RIF-1
+BSO

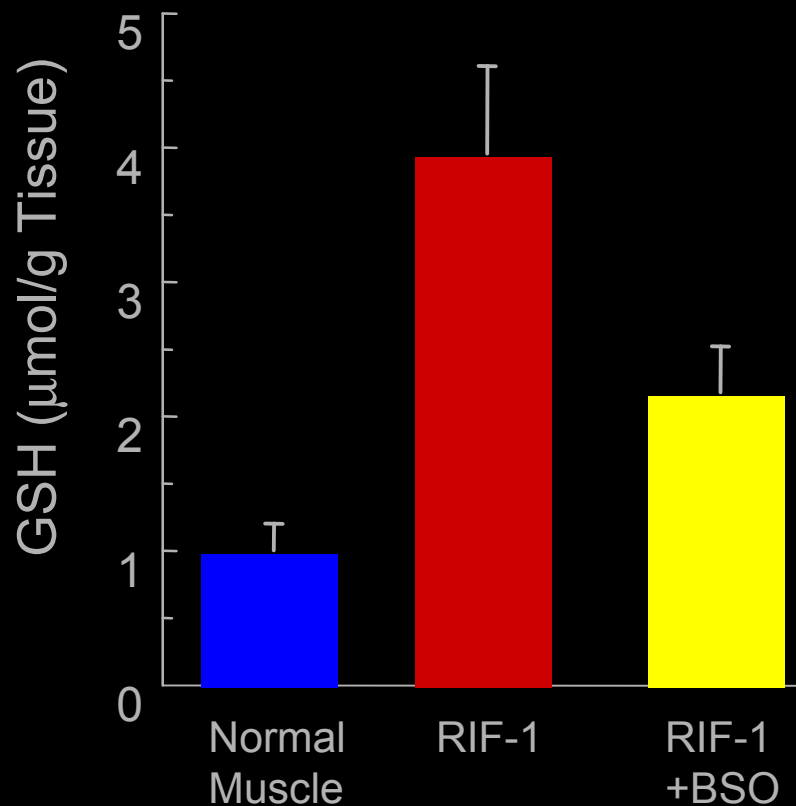


Median: 0.030 min⁻¹

0.0 0.05 0.10 0.15
Rate constant (min⁻¹)

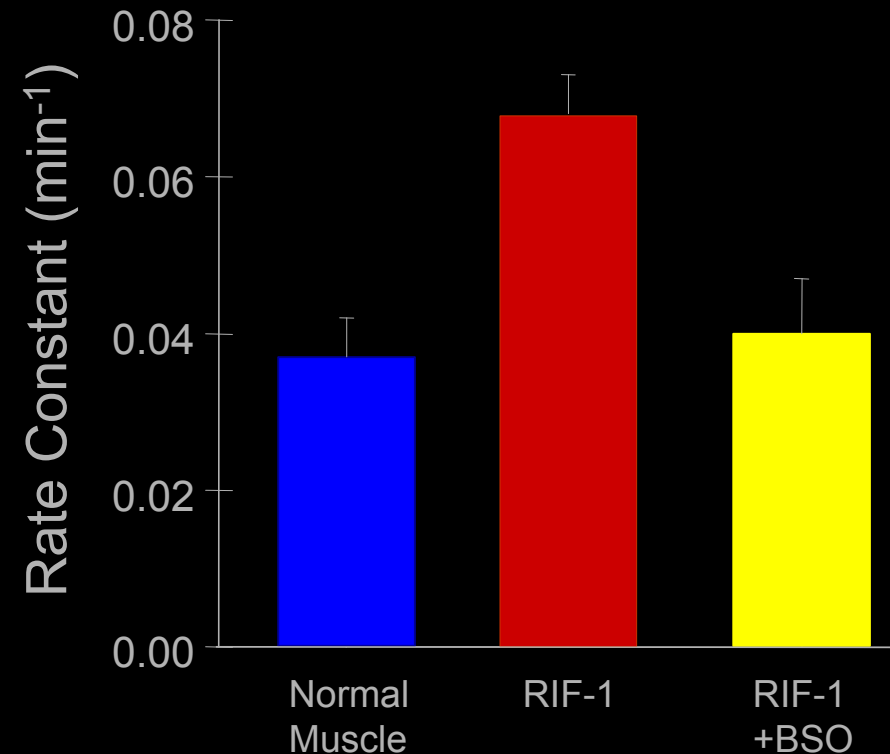
REDOX STATUS & GSH LEVELS IN RIF-1 TUMOR

GSH Level



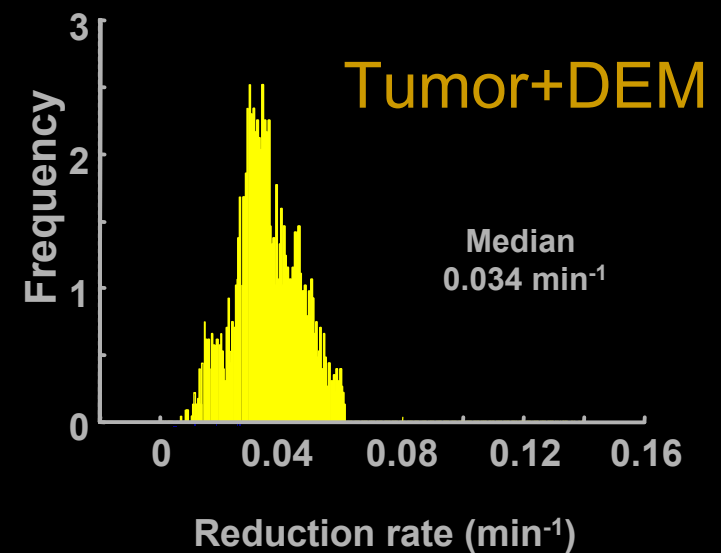
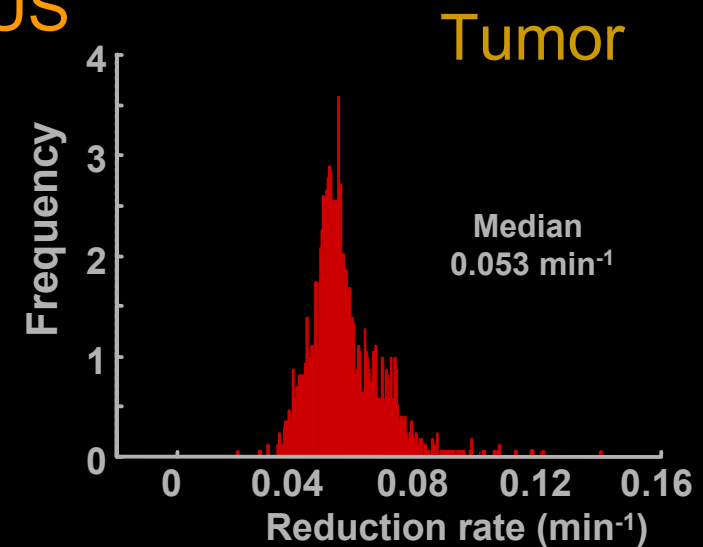
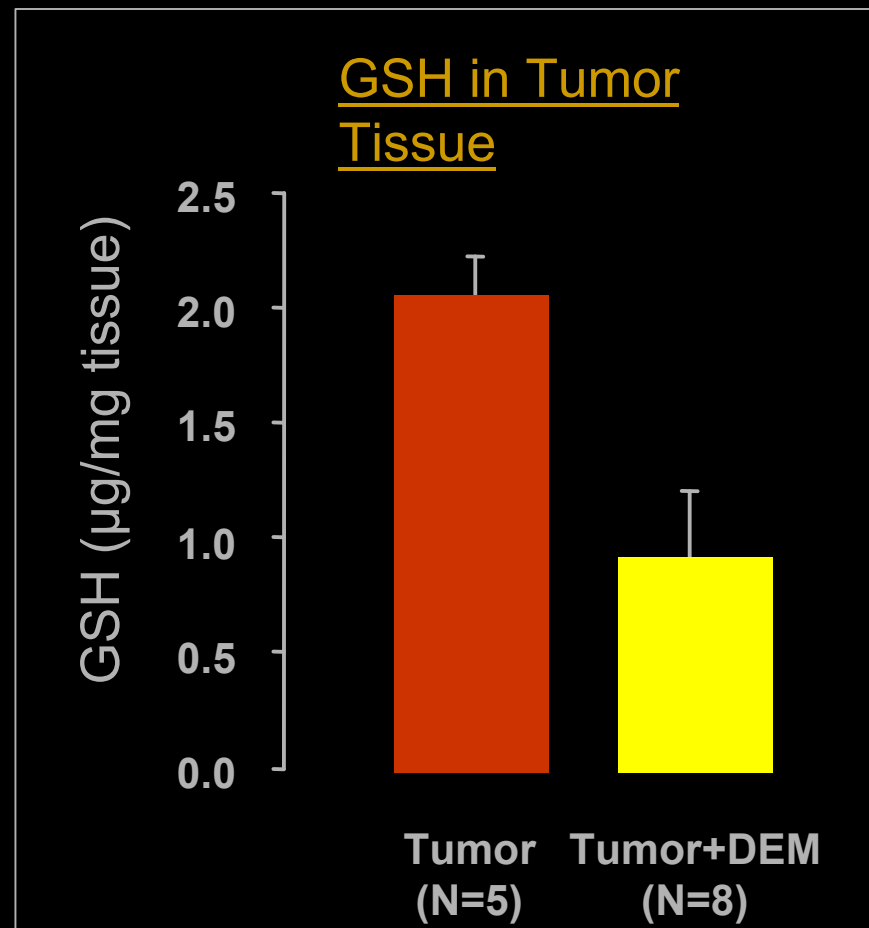
GSH levels in leg muscle (Normal) and RIF-1 tumors of untreated and BSO-treated (6-hrs post-treatment of 2.25 mmol/kg of BSO, *ip*) tumor-bearing mice. (N=7)

Redox Status



Rate constants of nitroxide clearance in leg muscle (Normal) and RIF-1 tumors of untreated and BSO-treated (6-hrs post-treatment of 2.25 mmol/kg of BSO, *ip*) tumor-bearing mice. (N=5)

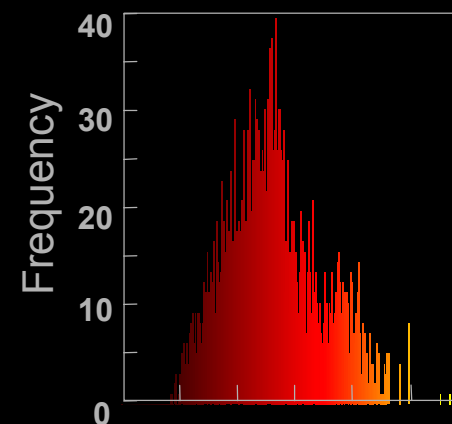
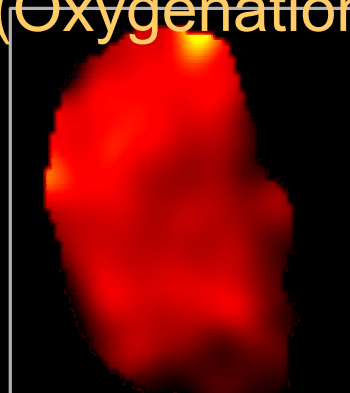
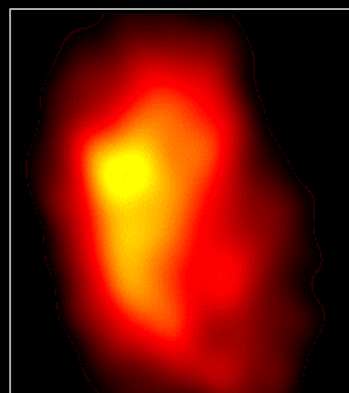
EFFECT OF DIETHYLMALEATE (DEM) ON TUMOR REDOX STATUS



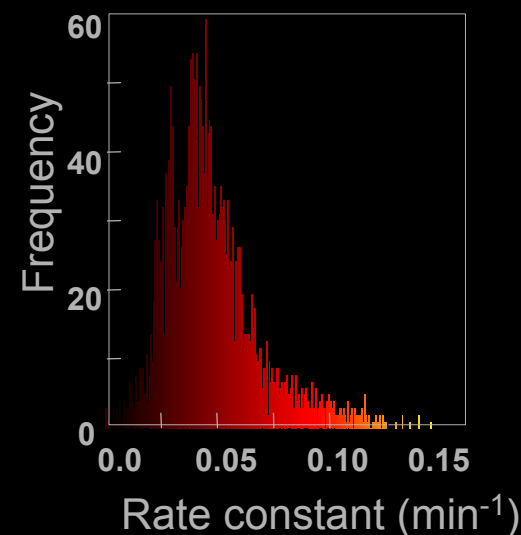
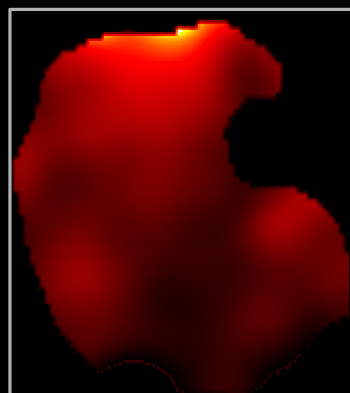
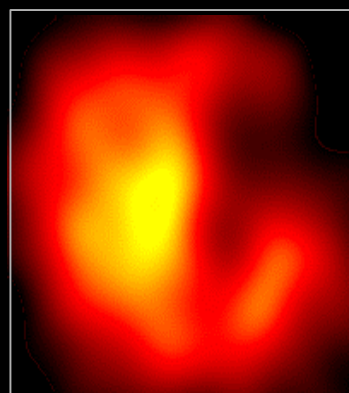
Yamada et al Acta Radiol (2002)

Redox mapping of tumor: Effect of Carbogen-Breathing (Oxygenation)

Room air



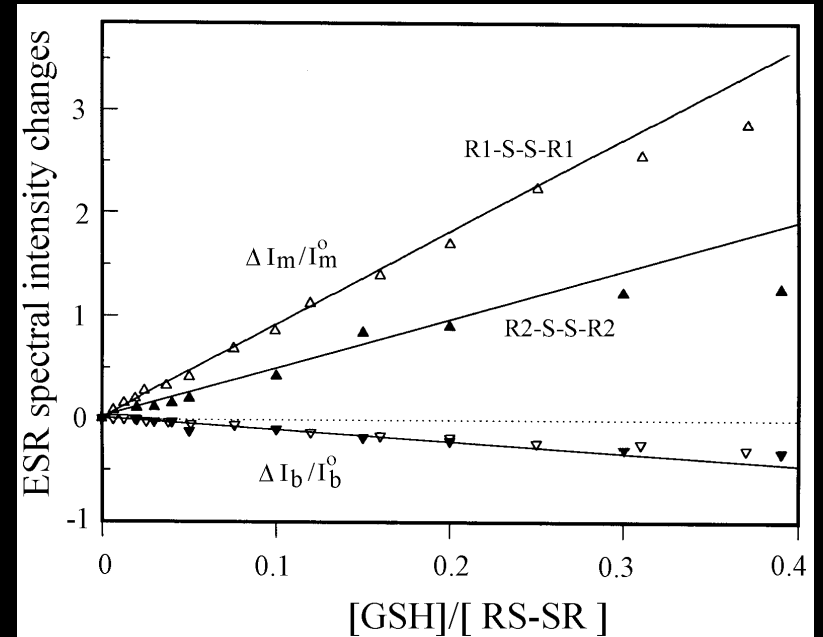
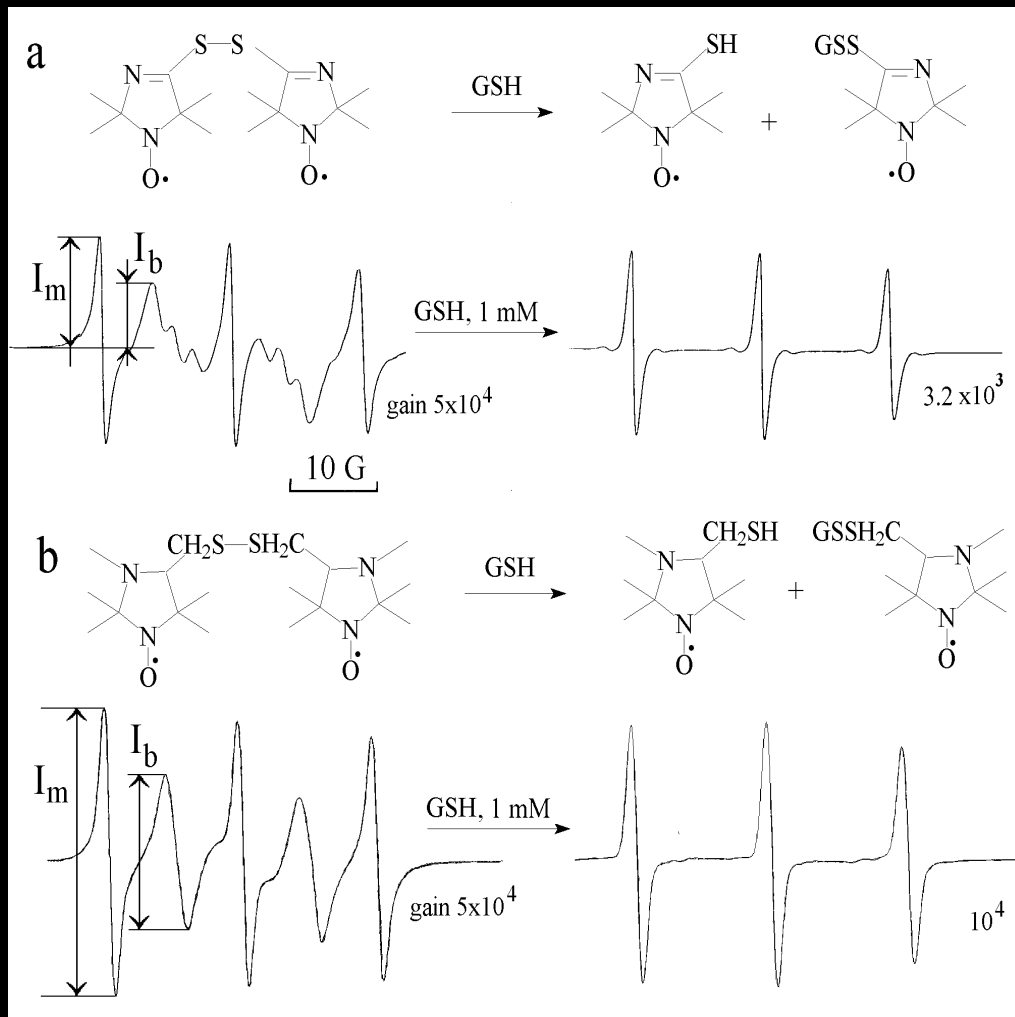
Carbogen



Nitroxide intensity -> 0.0 0.05 0.10 0.15
Rate constant (min^{-1})

EPR detection of SH-groups (ESR analogs of Ellman's reagent)

Reaction with GSH



Berliner, L.J., et al, Unique *In Vivo* Applications of Spin Traps, *Free Rad.Biol.Med.*30(5): 489-499.

Khramtsov, V.V. et al. 1997, *J.Biochem. Biophys. Methods* 35: 115

Summary

1. EPR spectroscopy is a direct & definitive technique for detection and quantitation of free radicals and paramagnetic species.
2. Low-frequency EPR spectroscopy enables measurement of free radicals (endogenous/exogenous) in biological systems including intact tissues, isolated organs and small animals.
3. *In vivo* EPR spectroscopy and imaging methods enable noninvasive measurement and mapping of tissue pO_2 , redox status and pH.

BOOKS

Rosen, G. M., Britigan, B. E., Halpern, H. J., and Pou, S. Free Radicals: Biology and Detection by Spin Trapping. New York: Oxford University Press, 1999.

Eaton, G. R., Eaton, S. S., and Ohno, K. EPR imaging and in vivo EPR: CRC Press, Inc, 1991.

REFERENCES

Buettner, G. R. Spin trapping: ESR parameters of spin adducts. *Free Radic Biol Med*, 3: 259-303, 1987.

Berliner, L. J., Khramtsov, V., Fujii, H., and Clanton, T. L. Unique in vivo applications of spin traps. *Free Radic Biol Med*, 30: 489-499, 2001.

McCay, P. B. Application of ESR spectroscopy in toxicology. *Arch Toxicol*, 60: 133-137, 1987.

Kuppusamy, P., Chzhazhan, M., Vij, K., Shteynbuk, M., Lefer, D. J., Giannella, E., and Zweier, J. L. Three-dimensional spectral-spatial EPR imaging of free radicals in the heart: a technique for imaging tissue metabolism and oxygenation. *Proc Natl Acad Sci U S A*, 91: 3388-3392, 1994.

Kuppusamy, P., Ohnishi, S. T., Numagami, Y., Ohnishi, T., and Zweier, J. L. Three-dimensional imaging of nitric oxide production in the rat brain subjected to ischemia-hypoxia. *J Cereb Blood Flow Metab*, 15: 899-903, 1995.

Kuppusamy, P., Wang, P., and Zweier, J. L. Three-dimensional spatial EPR imaging of the rat heart. *Magn Reson Med*, 34: 99-105, 1995.

Kuppusamy, P., Chzhazhan, M., Wang, P., and Zweier, J. L. Three-dimensional gated EPR imaging of the beating heart: time-resolved measurements of free radical distribution during the cardiac contractile cycle. *Magn Reson Med*, 35: 323-328, 1996.

Kuppusamy, P., Wang, P., Samouilov, A., and Zweier, J. L. Spatial mapping of nitric oxide generation in the ischemic heart using electron paramagnetic resonance imaging. *Magn Reson Med*, 36: 212-218, 1996.

Kuppusamy, P., Wang, P., Zweier, J. L., Krishna, M. C., Mitchell, J. B., Ma, L., Trimble, C. E., and Hsia, C. J. Electron paramagnetic resonance imaging of rat heart with nitroxide and polynitroxyl-albumin. *Biochemistry*, 35: 7051-7057, 1996.

Khramtsov, V. V., Yelinova, V. I., Glazachev Yu, I., Reznikov, V. A., and Zimmer, G. Quantitative determination and reversible modification of thiols using imidazolidine biradical disulfide label. *J Biochem Biophys Methods*, 35: 115-128, 1997.

Kuppusamy, P., Afeworki, M., Shankar, R. A., Coffin, D., Krishna, M. C., Hahn, S. M., Mitchell, J. B., and Zweier, J. L. In vivo electron paramagnetic resonance imaging of tumor heterogeneity and oxygenation in a murine model. *Cancer Res*, 58: 1562-1568, 1998.

- Kuppusamy, P., Shankar, R. A., and Zweier, J. L. In vivo measurement of arterial and venous oxygenation in the rat using 3D spectral-spatial electron paramagnetic resonance imaging. *Phys Med Biol*, 43: 1837-1844, 1998.
- Velan, S. S., Spencer, R. G., Zweier, J. L., and Kuppusamy, P. Electron paramagnetic resonance oxygen mapping (EPROM): direct visualization of oxygen concentration in tissue. *Magn Reson Med*, 43: 804-809, 2000.
- Kuppusamy, P., Shankar, R. A., Roubaud, V. M., and Zweier, J. L. Whole body detection and imaging of nitric oxide generation in mice following cardiopulmonary arrest: detection of intrinsic nitrosoheme complexes. *Magn Reson Med*, 45: 700-707, 2001.
- Ilangovan, G., Li, H., Zweier, J. L., Krishna, M. C., Mitchell, J. B., and Kuppusamy, P. In vivo measurement of regional oxygenation and imaging of redox status in RIF-1 murine tumor: Effect of carbogen-breathing. *Magn Reson Med*, 48: 723-730, 2002.
- Kuppusamy, P., Li, H., Ilangovan, G., Cardounel, A. J., Zweier, J. L., Yamada, K., Krishna, M. C., and Mitchell, J. B. Noninvasive imaging of tumor redox status and its modification by tissue glutathione levels. *Cancer Res*, 62: 307-312, 2002.
- Yamada, K. I., Kuppusamy, P., English, S., Yoo, J., Irie, A., Subramanian, S., Mitchell, J. B., and Krishna, M. C. Feasibility and assessment of non-invasive in vivo redox status using electron paramagnetic resonance imaging. *Acta Radiol*, 43: 433-440, 2002.

WEB SITES

The Illinois EPR Research Center: <http://ierc.scs.uiuc.edu/>

The National Biomedical EPR Center at the Medical College of Wisconsin :
<http://www.biophysics.mcw.edu/bri-epr/bri-epr.html>

NIEHS - Spin Trap Database: <http://epr.niehs.nih.gov/stdb.html>